Mon. Not. R. astr. Soc. (1968) **138**, 143–179.

THE ABUNDANCES OF THE ELEMENTS IN THE SOLAR PHOTOSPHERE—I

CARBON, NITROGEN AND OXYGEN

*D. L. Lambert**

(Received 1967 June 26)

Summary

This paper discusses the determination of the abundances of carbon, nitrogen and oxygen in the solar atmosphere from an analysis of atomic and molecular spectra. A detailed discussion of the neutral atomic spectra is presented. Five molecular bands are considered: C_2 Swan Band, CN red and violet systems, CO first overtone bands, and the CH ($A^2\Delta$–$X^2\Pi$) band. With the exception of the CH band, the analysis of the molecular bands yields abundances which are in good accord with the results from the neutral atomic spectra. The following abundances are derived:

log $A_C = 8{\cdot}55$, log $A_N = 7{\cdot}93$ and log $A_O = 8{\cdot}77$ on the standard scale log $N_H = 12{\cdot}00$.

General Introduction

1. *Introduction.* In 1960 Goldberg, Müller & Aller (1960) (subsequently referred to as GMA) published an abundance analysis for the solar photosphere. This fine contribution provides a frame of reference for the present series of papers. In this series the solar abundances will be revised and extended by incorporating the continuing advances in all fields relevant to abundance determinations: the revision and extension of laboratory spectrum analyses; the improvements in theoretical and experimental determinations of oscillator strengths; the increased accuracy of solar line profiles and equivalent widths resulting from photoelectric scanning; and the improvements in the model solar atmosphere.

In this paper, the abundances of carbon, nitrogen, and oxygen are discussed. GMA determined the abundances from the neutral atomic spectra but no attempt was made to derive abundances from the various molecular bands present in the solar spectrum. The rectification of this omission is a principal feature of this paper.

Problems, which are common to the interpretation of both atomic and molecular spectra, are discussed at the beginning of the paper: the model atmosphere, sources of equivalent widths, theory of line formation, and the effect of carbon monoxide formation. In Part II, an extensive rediscussion of the neutral spectra—C I, N I, O I—is presented. This is followed in Part III by the discussion of five molecular bands: C_2 Swan Band, CN red and violet systems, CO first overtone bands, and the CH ($A^2\Delta$–$X^2\Pi$) band. Part IV concludes the paper with an intercomparison of abundances derived from atomic and molecular spectra, a discussion of the effect on abundances of various uncertainties in the model atmosphere, and a discussion of the recommended abundances.

2. *Theory.* The theory of line formation is discussed in many papers and textbooks, see for example Aller (1963). The assumption of line formation by

*Present address: Mount Wilson and Palomar Observatories, Pasadena, California.

pure absorption was adopted throughout the calculations. A brief statement of the basic formulae will suffice.

For weak absorption lines, which are on the linear portion of the curve of growth, the equivalent width W_λ can be computed from the simple weighting function formula:

$$W_\lambda = \frac{\pi e^2}{m_e c^2} f\lambda^2 \int_0^\infty g_\lambda(\tau_0) \frac{N^*}{N_H} (1 - e^{-hc/\lambda kT}) \frac{d\tau_0}{\kappa_0} \qquad (2.1)$$

where κ_0 = the continuous absorption coefficient at $\lambda = 5000$ Å and per neutral hydrogen atom;
$g_\lambda(\tau_0)$ = the weighting function for pure absorption;
N^* = the number density of absorbing atoms or molecules;
N_H = the number density of neutral hydrogen atoms.

All other symbols are standard notation.

For atoms N^* is calculated from the Boltzmann and Saha equations. For carbon and oxygen an additional factor is included to account for the depletion of free carbon and oxygen through the formation of carbon monoxide, see Section 3.

Schadee (1964) has shown how N^* for a molecule may be expressed in terms of the partial pressures of the constituent atoms rather than the partial pressure of the molecule. The advantage of this method is that the complicated partition function for the molecule disappears from the expression. The correct use of the statistical weights in the Boltzmann equation is discussed further by Schadee (1967).

The weighting function method can be adapted for the treatment of medium-strong lines. However, the alternative method was preferred in which the emergent intensity in the line and the continuum is computed by direct numerical integration. The residual intensity in the line is given by

$$r_{\Delta\lambda} = \frac{\int_0^\infty B_\lambda(\tau_0) e^{-t_{\Delta\lambda}} dt_{\Delta\lambda}}{\int_0^\infty B_\lambda(\tau_0) e^{-\tau_\lambda} d\tau_\lambda} \qquad (2.2)$$

where τ_λ = optical depth in the continuum at the line centre;
$t_{\Delta\lambda}$ = total optical (line plus continuum) at a distance $\Delta\lambda$ from the line centre.

The equivalent width is calculated by a further integration over the line profile:

$$W_\lambda = \int_{-\infty}^{+\infty} (1 - r_{\Delta\lambda}) d\Delta\lambda. \qquad (2.3$$

Details of this method are provided by Aller (1963).

The application of the theory was straightforward. For selected multiplets th required portion of a curve of growth was computed via equations (2.2) and (2.3 Line damping (radiative, Stark, and van der Waals) was taken into account. uniform microturbulence of 1·8 km/s was assumed. The predicted and observe equivalent widths were displayed on a plot of log W_λ/λ vs log gf. The predictio were based on the GMA abundance so that the shift along the log gf axis require to achieve coincidence between the predictions and observations gave the correctic to the GMA abundance. Throughout the paper the units of W_λ/λ are W_λ in m and λ in microns.

The weighting function method was used primarily to compute equivalent widths of weak molecular lines. For weak atomic lines equations (2.2) and (2.3) were preferred since Mugglestone & O'Mara (1965) showed that saturation effects affect the equivalent width of high excitation lines even though the line is apparently weak.

The following notation for the abundance is used. If $N(\alpha)$ denotes the total number of atoms of species α, the abundance A_α is $A_\alpha = N(\alpha)/N(\mathrm{H})$. A_α is commonly expressed in logarithms to the base ten with $\log N(\mathrm{H}) = 12{\cdot}00$. For comparison purposes, the quantity $[\alpha]$ is introduced:

$$[\alpha] = \log A_\alpha/\mathrm{Lambert} - \log A_\alpha/\mathrm{GMA}. \qquad (2.4)$$

The GMA abundances for the three elements were

$$\log A_\mathrm{C} = 8{\cdot}72$$
$$\log A_\mathrm{N} = 7{\cdot}98$$
$$\log A_\mathrm{O} = 8{\cdot}96.$$

3. *Carbon monoxide formation.* In published papers concerned with the solar abundance of carbon, nitrogen and oxygen the assumption—rarely explicit—is made that the partial pressure of free atoms is not appreciably reduced by the formation of molecules. Molecular formation—initially CO and N_2—is considered significant only for stars of later spectral type than the Sun. The assumption may be justified by reference to the molecular equilibria calculations performed by de Jager & Neven (1957) which were based on dissociation constants calculated by Pecker & Peucheot (1957). Tsuji (1964) recalculated the dissociation constant for CO and obtained values which were between 10^{-2} to 10^{-3} of those given by Pecker & Peucheot. These revised calculations enhance considerably the depleting effect of carbon monoxide. Sample calculations indicated that even at photospheric temperatures the carbon monoxide is important if accurate abundances are desired The partial pressure of nitrogen is not reduced significantly by N_2 formation at photospheric temperatures.

The reduction in the partial pressure of carbon resulting from carbon monoxide formation is displayed in Fig. 1 for two model solar atmospheres: (i) see Table I,

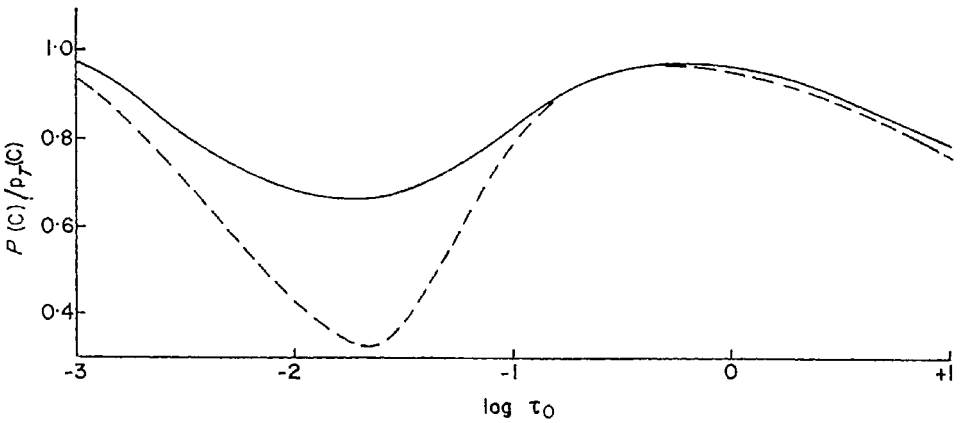

FIG. 1. *A plot of the ratio of the partial to total pressure of carbon as a function of optical depth for two model atmospheres:* ——— *see Table I,* – – – – *Utrecht Reference Photosphere.*

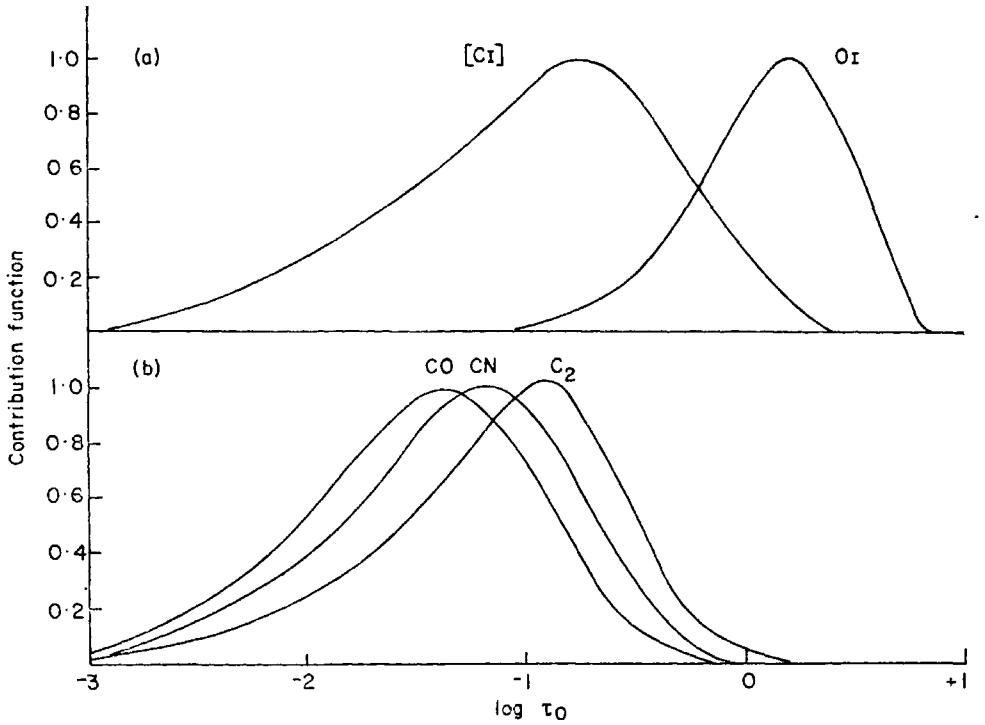

FIG. 2. *Contribution functions for some typical lines. Fig.* 2(a) *shows the contribution functions for the forbidden C* I *line* (λ8727 Å, *with* χ_{exc} = 1·27 *eV*) *and the permitted O* I *line* (λ6157 Å, χ_{exc} = 10·74 *eV*). *Fig.* 2(b) *gives the results for typical molecular lines CO* (λ23500 Å, χ_{exc} = 0·43 *eV*), *CN* (λ9500 Å, χ_{exc} = 0·33 *eV*) *and* C_2 (λ5150 Å, χ_{exc} = 0·18 *eV*).

(ii) the Utrecht Reference Photosphere (de Jager, Heintze & Hubenet 1964). Ionization of carbon which was also considered is responsible for the decreasing partial pressure at large optical depths. GMA abundances were assumed. The depletion of oxygen is approximately half that of carbon.

Contribution functions for [C I] λ8727 (see Section 6.3.3) and for some molecular lines are shown in Fig. 2. Clearly, for these lines carbon monoxide formation is important (compare Fig. 2 and Fig. 1). For example, for the adopted model atmosphere (Table 1) the predicted equivalent width of the [C I] line is reduced by 20 per cent when carbon monoxide is accounted for.

The above discussion applies to those lines which are formed in the outer layers of the photosphere: forbidden and strong permitted atomic lines and the molecular lines. The weak permitted lines of the neutral spectra are formed in the deepest layers of the photosphere. The contribution function of a typical line (O I λ6157 Å, χ_{exc} = 10·74 eV) is given in Fig. 2. For such lines carbon monoxide formation is unimportant.

4. *Model solar atmosphere.* The model solar atmosphere which was used in the current investigation is given in Table I. The temperature distribution $T(\tau_0)$ was derived following a detailed study of the solar continuous spectrum in the wavelength range 5000 Å to 13 microns and at disk positions cos $\theta \geqslant 0{\cdot}2$, (Lamber 1965). The gas and electron pressures were computed from the equation o hydrostatic equilibrium. The abundances of the dominant electron donors were taken from Lambert & Warner (1967). For these calculations microturbulenc

TABLE I

The model solar atmosphere

log τ_0	T(°K)	log Pg	log Pe
−4·0	4900	3·040	−0·902
−3·8	4900	3·157	−0·816
−3·6	4900	3·274	−0·728
−3·4	4900	3·389	−0·638
−3·2	4900	3·503	−0·547
−3·0	4900	3·616	−0·456
−2·8	4900	3·728	−0·363
−2·6	4730	3·838	−0·334
−2·4	4730	3·948	−0·240
−2·2	4730	4·056	−0·147
−2·0	4765	4·165	−0·043
−1·8	4780	4·274	+0·054
−1·6	4825	4·383	+0·161
−1·4	4895	4·493	+0·278
−1·2	5005	4·602	+0·409
−1·0	5140	4·711	+0·553
−0·8	5315	4·818	+0·719
−0·6	5555	4·919	+0·937
−0·4	5805	5·008	+1·182
−0·2	6100	5·085	+1·472
0·0	6435	5·147	+1·790
+0·2	6830	5·196	+2·136
+0·4	7315	5·234	+2·514
+0·6	7765	5·264	+2·828
+0·8	8115	5·292	+3·054
+1·0	8440	5·325	+3·281

Helium abundance: $A_{He} = 0{\cdot}09$.
Metal abundances: $A_{Si} = 3{\cdot}4 \times 10^{-5}$, $A_{Mg} = 3{\cdot}5 \times 10^{-5}$, $A_{Fe} = 6{\cdot}3 \times 10^{-6}$, $A_{Ca} + A_{Na} = 3{\cdot}8 \times 10^{-6}$.

was not included. The resulting slight error in the gas and electron pressures has a negligible effect on the abundances. A full discussion of the effect on the abundances of uncertainties in the model atmosphere is given in Section 14.2.

5. *Equivalent widths.* This investigation is based on equivalent width measurements obtained at the centre of the solar disk. The three principal sources of equivalent widths are:

(i) The Table of Solar Spectrum Wavelengths, 11984–25578 Å, Mohler (1955);
(ii) The Preliminary Photometric Catalogue of Fraunhofer Lines, λ3164–λ8770, Utrecht (1960);
(iii) The Photometric Atlas of the Solar Spectrum, λ7498–λ12016, Delbouille & Roland (1963).

Since there is no catalogue of equivalent widths for the Delbouille & Roland Atlas, equivalent widths were obtained by careful measurement of the Atlas tracings.

A number of other sources were consulted. Full details of these are given in the appropriate table containing the selected lines. These tables also give the adopted equivalent width as well as the individual values from the various sources.

Atomic Spectra

6. *The C I spectrum*

6.1 *Introduction.* A substantial increase in the number of identified C I lines in the solar spectrum was achieved as the direct result of the laboratory reinvestigations by Johansson (1963), and Johansson & Litzen (1965), and the subsequent revision of the term system by Johansson (1966). Approximately 100 C I lines were identified and were considered sufficiently free from blends for an abundance determination. Of these about 25 were new identifications and they included the forbidden line at $\lambda 8727{\cdot}14$ Å ($2p^2\ ^1D_2 - 2p^2\ ^1S_0$) (Lambert & Swings 1967a).

However, following a critical discussion of theoretical and experimental oscillator strengths (see Section 6.2) for the permitted lines only the $3s$–$3p$ transition array was selected for the abundance determination. In Table II, the lines selected from this array are listed. A full list of C I identifications together with solar gf values will be presented in a later paper.

6.2 *Oscillator strengths.* Since errors in the oscillator strength affect directly the derived abundance a full discussion of theoretical and experimental oscillator strengths is presented.

TABLE II

C I spectrum: 3s–3p transition array

Multiplet	ΔJ	λ(Å)*	χ (eV)	log gf †	W_λ‡	log W_λ/λ§	Remarks‖
$^3P^0$–^3D	2–3	10691·24	7·49	+0·33	310	2·46	310L, 347J, 281M, 255A
	2–2	10729·59	7·49	−0·42	175	2·21	171L, 190J, 162M, 177A
	2–1	10754·02	7·49	−1·59	45	1·62	43L, 58M
	1–2	10683·09	7·48	+0·06	248	2·37	247L, 250J, 205A
	1–1	10707·36	7·48	−0·42	170	2·20	168L, 176J, 170M, 145A
	0–1	10685·36	7·48	−0·29	190	2·25	184L, 195J, 189M, 164A
$^3P^0$–^3P	2–2	9094·82	7·49	+0·14	240	2·42	242L, 226A
	2–1	9111·88	7·49	−0·33	170	2·27	166L, 182M, 155A
	1–2	9061·44	7·48	−0·33	155	2·23	L
	1–1	9078·28	7·48	−0·57	125	2·14	126L, 116A
$^3P^0$–^3S	2–1	9658·40	7·49	−0·25	155	2·21	150L, 165M, 151A
	0–1	9603·14	7·48	−0·94	95	2·00	98L, 79: A
$^1P^0$–^1S	1–0	8335·15	7·69	−0·42	108	2·11	105L, 114PPC
$^1P^0$–^1D	1–2	9405·74	7·69	+0·27	210:	2·35	210L, 177A

* Solar wavelengths from Babcock & Moore (1947).

† Coulomb approximation gf values.

‡ W_λ is the adopted equivalent width in mÅ. : denotes an uncertain result.

§ W_λ in mÅ and λ in microns.

‖ The W_λs from various sources are listed: L = Delbouille & Roland (1963), J = de Jag & Neven (1964), A = Allen (1938), M = McMath Hulbert observations quoted by GM PPC = Preliminary Photometric Catalogue, Utrecht (1960).

The Coulomb approximation method (Bates & Damgaard 1949), is expected to give reliable oscillator strengths for carbon, nitrogen, and oxygen. Indeed, it is the only theoretical method that has been applied extensively to the C I spectrum. The Coulomb approximation provides only the radial integral (σ^2 in standard notation). To calculate the oscillator strengths the multiplet and line strengths (S(M) and S(L) respectively) are required. When LS coupling dominates S(M) and S(L) are readily calculable and Aller (1963) gives convenient tables for these quantities. Unfortunately, inspection of the C I term diagram shows that for only two configurations—$2s^2 3p 3s$ and $2s^2 2p 3p$—are the term separations in fair agreement with the Lande interval rule. Therefore, LS coupling is not generally applicable. Johansson (1966) shows that this failure is the result of spin–orbit interactions. The evaluation of the line strengths in intermediate coupling has not been attempted. The theoretical oscillator strengths are applicable only to the $3s$–$3p$ transition array for which LS line and multiplet strengths should be valid.

Three series of oscillator strength measurements are available for high excitation lines in the visible and infra-red: Maecker (1953), Richter (1958) and Foster (1962). The internal accuracy for these measurements appears satisfactory but the reliability of their absolute scales is in doubt.

The source in each case was a stabilized arc run in a mixture of gases. The plasma composition must be known in order to calculate the density of carbon atoms. In each investigation the assumption was made that the composition was uniform and equal to that of the inflowing gas mixture. Detailed studies of inhomogeneous arcs show that the plasma has a non-uniform composition (Maecker (1956), Mastrup & Wiese 1958). A correction for non-uniformity is difficult to apply. Wiese, Smith & Glennon (1966) suggest that the published oscillator strengths be considered as relative measurements and that their absolute scale be determined by reference to the Coulomb approximation results.

Experimental and theoretical (Coulomb approximation) oscillator strengths are compared in Table III. Total gf values for a multiplet are tabulated.

There is an almost constant difference in log gf between the theoretical values and Richter's extensive set of experimental measurements. It was argued previously that the breakdown of LS coupling limits the validity of the theoretical oscillator strengths to the $3s$–$3p$ array. According to the differences in log gf_t for this array Richter's results should be multiplied by a factor $1{\cdot}4 \pm 0{\cdot}1$ to place them on the absolute scale.

Since an accurate abundance is obtained from the $3s$–$3p$ array, the experimental results for other arrays were not used. However, a comparison (see Section 6.3.1 and Fig. 5) does indicate that the normalized experimental results are to be preferred over the theoretical values. Of the transitions in Table III, $3p\,^1P$–$4s\,^1P$ is the most striking example. The gf value deduced from the equivalent width and a carbon abundance is in good agreement with the normalized experimental gf value.

6.3 *The carbon abundance*

6.3.1 *C I curves of growth.* The discussion on oscillator strengths anticipated a result first obtained from curves of growth for individual transition arrays. Figs 3 and 4 show the curves of growth for the $3p$–$3d$ and $3p$–$4d$ transition arrays which are obtained using the theoretical oscillation strengths. For $3p$–$3d$, curves of

TABLE III

gf values for C I multiplets

Transition array	Multiplet	λ(Å)	log gf_t* BD	R	M	F	Δ log gf_t (R–BD)
$3s$–$3p$	$^1P^0$–^1S	8336	−0·423	−0·51			−0·09
	$^1P^0$–^1D	9406	0·269	0·07			−0·20
	$^3P^0$–^3S	9630	0·010	−0·15			−0·15
	$^3P^0$–^3P	9080	0·505	0·33			−0·18
	$^3P^0$–^3D	10720	0·667	0·53			−0·14
$3s$–$4p$	$^1P^0$–^1S	4932	−1·621	−1·89	−2·26	−1·82	−0·27
	$^1P^0$–^1P	5380	−1·856	−1·78	−2·03	−1·82	+0·08
	$^1P^0$–^1D	5052	−1·285†	−1·60	−1·78	−1·59	−0·31
	$^3P^0$–^3S	4822	−2·099†			−2·10	
	$^3P^0$–^3P	4770	−1·244	−1·42	−1·80	−1·53	−0·18
$3s$–$5p$	$^1P^0$–^1D	4269	−1·959			−2·50	
$3p$–$4s$	^1P–$^1P^0$	10548	−0·497	−1·39			−0·89
	^3D–$^3P^0$	11850	0·321	0·22			−0·10
$3p$–$3d$	^1P–$^1P^0$	10124	−0·162	−0·17			−0·01
	^1P–$^1D^0$	11330	0·313	0·16			−0·15
	^1D–$^1F^0$	16890	0·570	0·45			−0·12
	^3S–$^3P^0$	11660	0·452	0·34			−0·11
	^3P–$^3P^0$	12600	0·335	0·25			−0·09
	^3D–$^3D^0$	11630	0·323	0·16			−0·16
	^3D–$^3F^0$	11760	1·070	0·87			−0·20

* BD = Bates & Damgaard (1949) Coulomb approximation, R = Richter (1958), M = Maecker (1954), F = Foster (1962).

† Severe cancellation exists in these transition integrals.

growth for individual multiplets are given. The displacement of the observed points from the curve is equal to the abundance correction [C], see equation (2.4). A composite curve of growth is given for $3p$–$4d$ array. It will be noticed that the average correction for a multiplet [C] ranges from about −1·0 to +0·2.

This large range in [C] occurs for both strong and weak lines so that the spread cannot be attributed to errors in the equivalent widths. Several examples can be found where multiplets of similar excitation potential and wavelength (e.g $3p^3D$–$3d^3P^0$, $3p^1P$–$3d^1P^0$) give very different abundances. This observation indicates that the model atmosphere is not responsible for the scatter. Even more significant is the absence of the multiplets $3p^1D$–$3d^1F^0$ and $3p^1D$–$4d^1F^0$. On the basis of LS multiplet strengths these transitions should be the strongest of the transitions between singlet levels. The conclusion is that the theoretical oscillator strengths (Coulomb approximation radial integrals plus LS line and multiplet strengths) are inadequate for many of the transitions in C I.

The abundance corrections [C] correlate well with the difference between the experimental and theoretical values for log *gf*. This is shown by Fig. 5. It would be possible to use the normalized experimental measurements to extend the abundance determination to include other transition arrays.

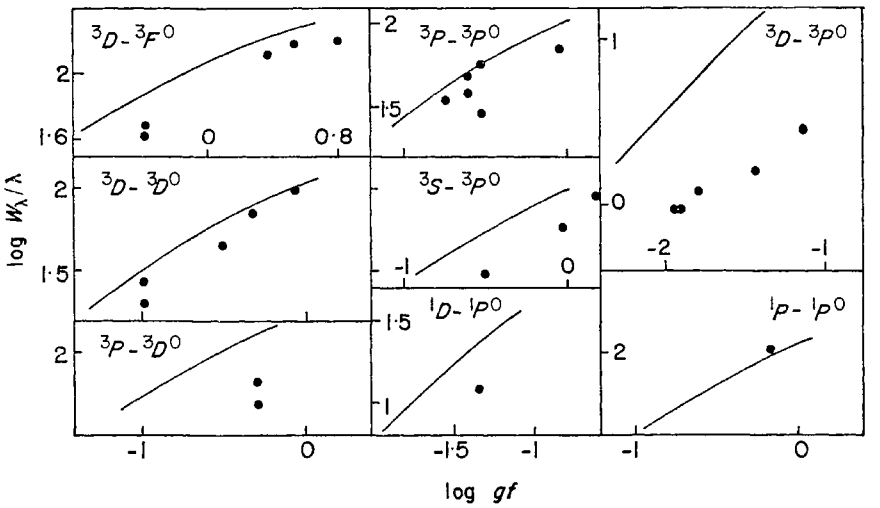

FIG. 3. *Curves of growth for multiplets from the transition array 3p–3d. The solid lines gives the predicted curve based on the GMA abundance for carbon. The displacement of the observed points along the log gf axis is equal to the abundance correction [C]. The mean value of [C] for each multiplet is as follows:*

^3D–$^3P^0$ [C] = −0·35; ^3D–$^3D^0$ [C] = −0·13; ^3P–$^3D^0$ [C] = −0·5;
^3P–$^3P^0$ [C] = −0·20; ^3S–$^3P^0$ [C] = −0·35; ^1D–$^1P^0$ [C] = −0·32;
^3D–$^3P^0$ [C] = −0·90; ^1P–$^1P^0$ [C] = +0·10.

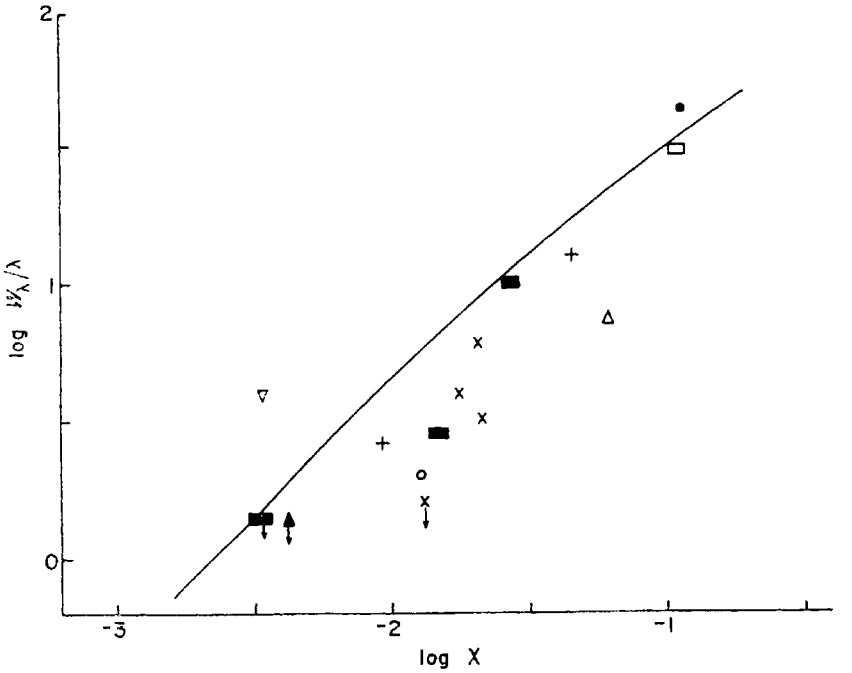

FIG. 4. *A composite curve of growth for the 3p–4d transition array for the multiplets:* ● ^3D–$^3F^0$, ■ ^3D–$^3D^0$, ▲ ^3D–$^3P^0$, × ^3P–$^3P^0$, + ^3S–$^3P^0$, ○ ^1D–$^1F^0$, □ ^1P–$^1P^0$ △ ^1P–$^1D^0$, *and* ▽ ^1S–$^1P^0$. *Arrowed symbols denote lines which are absent from the solar spectrum, and for which an upper limit to the equivalent width was estimated.*

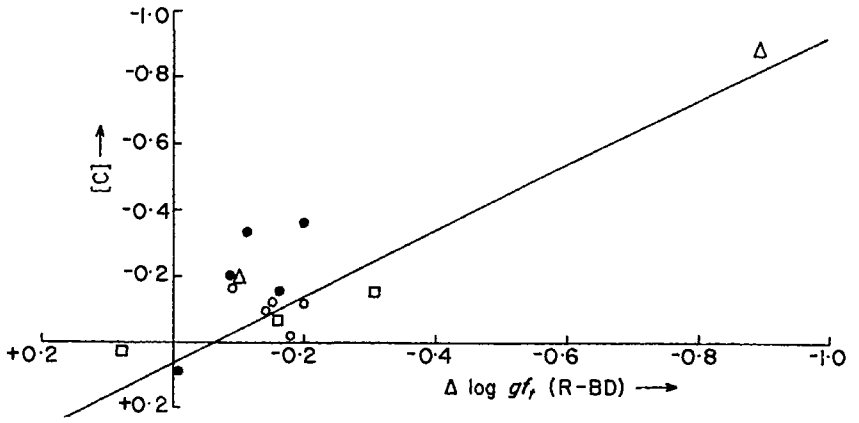

FIG. 5. *A comparison of the* [C] *with* Δ log gf_t(*R–BD*) *for the transition arrays:* ○ 3*s*–3*p*, □ 3*s*–4*p*, △ 3*p*–4*s*, *and* ● 3*p*–3*d*. *The solid line with unit slope demonstrates that the adoption of the experimental oscillator strengths would lead to a reduction in the spread of the* [C] *results for individual multiplets.*

There are two reasons for the failure of the theoretical oscillator strengths: first, LS-coupling breaks down; and second, for many of the Coulomb approximation transition integrals the positive and negative contributions are almost equal and strong cancellation results. Numerous examples of strong cancellation were found by examination of the dependence of transition integral on the effective quantum number n^*. Further, from the correlation of [C] with the distance $(n^*–n_0^*)$ from a node at n_0^*, a working rule was established: if $|n^*–n_0^*| > 0{\cdot}1$ then the coulomb approximation appears to give a satisfactory result. For the first array of a series the transition integrals have large positive values but for other arrays the working rule results in the rejection of about 80 per cent of the multiplets. The extent to which strong cancellation affects the C I transition integrals appears to have been overlooked in previous investigations. Finally, the calculations of line strengths in intermediate coupling will be of limited value until improved methods for the calculation of C I transition integrals are developed.

6.3.2 *The* 3*s*–3*p transition array.* The abundance determination was restricted to the 3*s*–3*p* transition array for which the theoretical oscillator strengths should be valid. Fourteen lines with good equivalent width measurements are listed in Table II. In the calculations of the line absorption coefficient line broadening was included. Van der Waals broadening provides the major contribution: estimates of the mean square radius $\overline{R^2}$ were obtained from the Coulomb approximation formula. Muggleton & O'Mara calculated the radiative damping constant Γ_{rad}, and the Stark broadening factor $\Delta\nu/E^2$. For transitions not included in their work, the parameter Γ_{rad} and $\Delta\nu/E^2$ were calculated from the standard expressions—see Aller (1963). The adopted constants and coulomb approximation oscillator strengths are listed in Table IV.

Curves of growth were calculated for the five multiplets. Abundance corrections [C] for individual lines are given in Table IV. The mean result is

$$[C] = -0{\cdot}13 \pm 0{\cdot}03.$$

The scatter in the [C] values is small and should be contrasted with results for the 3*p*–3*d* array given in Fig. 3. The scatter in the 3*s*–3*p* results is entirely attributable to equivalent width measurement errors; for the strongest lines in the array an error of ±10 per cent in W_λ corresponds to ±0·15 in [C].

TABLE IV

C I: $3s$–$3p$ *transition array*

Multiplet	λ (Å)	$10^{-7}\,\Gamma_{rad}$	$10^{-12}\,\Delta\nu/E^2$	$\overline{R_u^2}/a_0^2$	$\overline{R_l^2}/a_0^2$	log gf	log W_λ/λ	[C]
$^3P^0$–^3D	10691·24	5·8	2·3	55	34	+0·33	2·46	−0·12
	10729·59					−0·42	2·21	−0·09
	10754·02					−1·59	1·62	−0·20
	10683·09					+0·06	2·37	−0·11
	10707·36					−0·42	2·20	−0·11
	10685·36					−0·29	2·25	−0·11
$^3P^0$–^3P	9094·82	6·7	0·80	65	34	+0·14	2·42	−0·04
	9111·88					−0·33	2·27	0·00
	9061·44					−0·33	2·23	−0·11
	9078·28					−0·57	2·14	−0·12
$^3P^0$–^3S	9658·40	6·4	2·0	61	34	−0·25	2·21	−0·26
	9603·14					−0·94	2·00	−0·10
$^1P^0$–^1S	8335·15	9·7	4·7	89	38	−0·42	2·11	−0·23
$^1P^0$–^1D	9405·74	9·0	3·0	75	38	+0·27	2·35	−0·22

Γ_{rad} in s^{-1}; $\Delta\nu$ in cm^{-1}, E in volts; $\overline{R^2}$ is the mean square radius: u = upper, l = lower level; a_0 = atomic unit.

6.3.3 *The forbidden C* I *line,* λ8727·14 Å. Solar identifications for [C I] lines from transitions within the $2s^22p^2$ ground configuration are proposed by Lambert & Swings (1967a). The only suitable line for abundance determinations is that (at λ8727·14 Å) arising from the transition $2p^2\ ^1D_2$–$2p^2\ ^1S_0$.

The equivalent width was measured from a scan obtained with the Kitt Peak spectrometer: $W_\lambda = 6{\cdot}5 \pm 0{\cdot}5$ mÅ.

Theoretical transition probabilities for this electric quadrupole transition are available. Garstang (1951) computed self-consistent field wave functions and obtained $A = 0{\cdot}50\ s^{-1}$. Froese (1966) calculated Hartree–Fock wave function and her transition integral gives $A = 0{\cdot}650\ s^{-1}$. This latter value is probably the more accurate and is adopted.

With the adopted equivalent width and transition probability the abundance is given (for [O] = 0·00) by

$$[C] = -0{\cdot}19 \pm 0{\cdot}07.$$

The uncertainty in [C] is a rough estimate based on the possible error in the equivalent width and transition probability. The forbidden line gives an abundance about 15 per cent smaller than that from the strong C I lines.

6.3.4 *Discussion.* The essential differences between the present analysis and that by GMA should be summarized. First, line damping, which was assumed by GMA to be zero, was correctly taken into account in the calculations of the curves of growth. The omission of damping for the strong $3s$–$3p$ lines would increase the abundance by about 0·2 to 0·3 dex*. Second, the analysis was restricted

* 'dex' is equivalent to 'in the ten-based logarithm'.

to the $3s$–$3p$ array because of the evidence that the theoretical oscillator strengths for the other arrays are unreliable. Third, the recent identification of the [C I] line at $\lambda 8727$ Å provides a welcome check on the permitted lines.

A discussion on the recommended carbon abundance is postponed until Sections 14 and 15.

7. *The N I spectrum*

7.1 *Introduction.* Table V lists the 14 N I lines used for the abundance determination. It also includes two lines for which an upper limit to the equivalent width has been given. Five lines are believed to be new solar identifications. They were the result of a search based on the laboratory wavelengths obtained by Eriksson (1958). In seven cases, the N I line is blended with a line of the CN red system (Davis & Phillips 1963). The equivalent width of the CN blend was computed (Lambert 1967a) and subtracted from the observed equivalent width. The list contains eight of the ten lines used by GMA, two were rejected on account of severe blending.

Houziaux (1961) proposed a solar identification for the infrared [N I] doublet. Lambert & Swings (1967b) show that this identification is very doubtful.

TABLE V

N I lines in the solar spectrum

Transition	ΔJ	λ_{air} (Å)†	χ (eV)	log gf ‡ CA	log gf ‡ NBS	W_λ	log W_λ/λ	Remarks§‖
$3s\ ^4P$–$3p\ ^4D^0$	$\frac{3}{2}$–$\frac{5}{2}$	8683·40	10·33	+0·11	−0·05	7·1	0·91	8·0L, 8PPC *CN
	$\frac{5}{2}$–$\frac{5}{2}$	8718·83	10·34	−0·26	−0·43	4·5:	0·71	45L, 5P
	$\frac{3}{2}$–$\frac{3}{2}$	8711·70	10·33	−0·18	−0·34	4·5	0·71	4·5L, 4·5M, 4·5PPC
	$\frac{1}{2}$–$\frac{1}{2}$	8703·25	10·33	−0·29	−0·41	3·0	0·54	4·4L, 5M, 8PPC *CN
$3s\ ^4P$–$3p\ ^4P^0$	$\frac{3}{2}$–$\frac{5}{2}$	8184·87	10·33	−0·23	−0·42	3·6	0·64	5·0L *CN
	$\frac{5}{2}$–$\frac{5}{2}$	8216·35	10·34	+0·13	−0·01	6·9	0·92	6·9L, 7PPC
$3s\ ^4P$–$3p\ ^4P^0$	$\frac{3}{2}$–$\frac{3}{2}$	7442·30	10·33	−0·33	−0·45	2·7	0·56	3PPC *CN
	$\frac{5}{2}$–$\frac{3}{2}$	7468·31	10·34	−0·16	−0·27	4	0·73	PPC
$3s\ ^2P$–$3p\ ^2D^0$	$\frac{3}{2}$–$\frac{5}{2}$	9392·79	10·69	+0·31	+0·24	7·6	0·91	9·4L *CN, new
$3s\ ^2P$–$3p\ ^2P^0$	$\frac{1}{2}$–$\frac{1}{2}$	8594·01	10·68	−0·32	−0·38	2·5:	0·46	3·7L *CN, new
	$\frac{3}{2}$–$\frac{3}{2}$	8629·24	10·69	+0·08	+0·03	4·9:	0·75	6·6L, 5M, 6PPC *CN
	$\frac{3}{2}$–$\frac{1}{2}$	8655·87	10·69	−0·62	−0·65	1·5★	0·24	L
$3p\ ^4D^0$–$3d\ ^4F$	$\frac{5}{2}$–$\frac{7}{2}$	10112·48	11·76	+0·58	+0·60	2·8:	0·44	L new
	$\frac{7}{2}$–$\frac{9}{2}$	10114·64	11·76	+0·74	+0·76	4·1	0·61	L new
	$\frac{3}{2}$–$\frac{5}{2}$	10108·89	11·75	+0·39	+0·41	1·5★	0·17	L
$3p\ ^4P^0$–$3d\ ^4D$	$\frac{5}{2}$–$\frac{7}{2}$	10539·57	11·84	+0·52	+0·51	2·2:	0·32	L new

★ Upper limit.
† From Eriksson (1958).
‡ CA = Coulomb approximation, NBS = Wiese, Smith, Glennon (1966).
§ See Table II.
‖ *CN denotes a blend with a CN line, see text; new = new identification.

7.2 *Oscillator strengths.* Richter (1961) measured emission line intensities from a stabilized arc source and obtained oscillator strengths for the multiplets listed in Table V. An uncertainty of only 10 to 15 per cent is claimed. The arc was run in almost pure nitrogen and, therefore, the adverse criticism proposed during the discussion on C I oscillator strength measurements is inapplicable.

Coulomb approximation results are expected to be reliable for nitrogen. However Wiese, Smith & Glennon (1966) state that for the $3s$–$3p$ array the transition integral is subject to strong cancellation. The variation of the transition integral with the effective quantum number for the $3p$ levels was examined. There was no indication that strong cancellation occurs in the $3s$–$3p$ integrals. Departures from LS coupling for the $3d$ configuration are indicated by the term diagram and this may affect the theoretical line strengths.

Hartree–Fock–Slater calculations of the radial integral are available (Kelly 1964). Petrie (1950) estimated the oscillator strength for the multiplet $3s\,^4P$–$3p\,^4D^0$ from hydrogen-like wave functions. Varsavsky (1958) used the charge-expansion method to calculate oscillator strengths for $3s\,^4P$–$3p\,^4D^0$ and $3p\,^4D^0$–$3d\,^4F$.

The experimental and theoretical oscillator strengths are compared in Table VI. The recommended values from the recent N.B.S. compilation ' Atomic Transition Probabilities ' (Wiese, Smith & Glennon 1966), which are also listed, are weighted in favour of the experimental results.

The Coulomb approximation predictions for the $3s$–$3p$ array are 25 per cent larger and for $3p$–$3d$ 4 per cent smaller than the experimental results. The origin of this discrepancy cannot be identified. The large difference for the $3s$–$3p$ array is probably attributable to an error in the absolute scale of the experimental results. The reduced difference for $3p$–$3d$ could be attributed to either departures from LS coupling in the $3d$ configuration or to a systematic error in the experimental results which was a function of wavelength or excitation potential.

The Coulomb approximation is adopted because of the great difficulties in establishing an accurate absolute scale for the experimental oscillator strengths. Accurate solar equivalent widths could be used to test this choice by providing an independent measurement of the ratio of multiplet oscillator strengths in the $3s$–$3p$ and $3p$–$3d$ arrays. The present observations are not sufficiently accurate for this purpose.

TABLE VI

gf values for N I multiplets

Transition array	Multiplet	λ (Å)	log gf_t*						Δ log gf_t (R–BD)
			R	BD	K	P	V	NBS	
$3s$–$3p$	^4P–$^4D^0$	8680	0·63	0·79	0·85	0·62	0·63	0·63	−0·16
	^4P–$^4P^0$	8216	0·52	0·59	0·66			0·443	−0·07
	^4P–$^4S^0$	7478	0·01	0·14	0·22			0·025	−0·13
	^2P–$^2P^0$	8629	0·28	0·33	0·33			0·281	−0·05
	^2P–$^2D^0$	9393	0·46	0·53	0·52			0·458	−0·07
$3p$–$3d$	$^4D^0$–^4F	10115	1·23	1·19	1·20		1·15	1·205	0·04
	$^4P^0$–^4D	10540	0·92	0·92	0·91			0·917	0·00

* R = Richter (1961), BD = Bates & Damgaard (1949), K = Kelly (1964), P = Petrie (1950), V = Varsavsky (1958), NBS = Wiese, Smith, Glennon (1966).

7.3 *The nitrogen abundance.* A curve of growth was computed for each multiplet. A composite curve of growth was constructed (see Fig. 6). The simple weighting function method was not used because saturation effects for apparently weak N I lines cannot be assumed negligible (Mugglestone & O'Mara 1965).

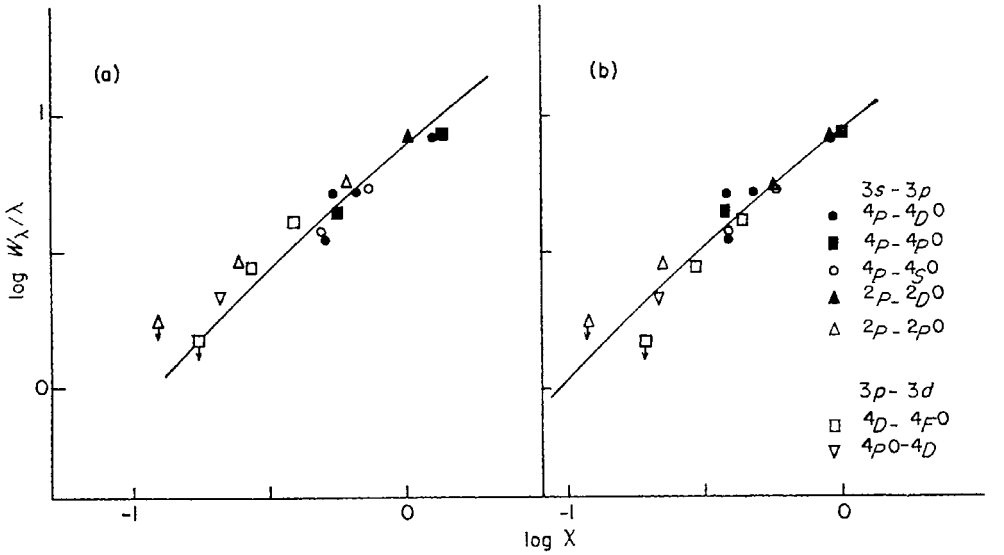

FIG. 6. *Curves of growth for N I lines from the 3s–3p and 3p–3d transition arrays constructed using in Fig.* 6(a) *the theoretical and in Fig.* 6(b) *the experimental (NBS) oscillator strengths. The solid line represents in each case the best fitting curve of growth.*

With the theoretical oscillator strengths (Coulomb approximation radial integrals plus LS line strengths) the mean nitrogen abundance is

$$\log A_N = -4{\cdot}03 \text{ or } [N] = -0{\cdot}01.$$

If the NBS (or experimental) oscillator strengths are preferred [N] is increased to $+0{\cdot}10$. The scatter in the [N] for individual lines suggests an error of about $\pm 0{\cdot}05$.

GMA suggested that the two lines at $\lambda 7400$ Å gave a significantly large abundance. This is not confirmed in Fig. 6. Their conclusion was the consequence of an error in their Coulomb approximation oscillator strengths.

The GMA and the present nitrogen abundance are almost identical. This is attributable to the common use of the coulomb approximation and to the fact that the model atmospheres have very similar temperature distributions in the deep layers $\log \tau_0 > 0{\cdot}0$.

8. *The O I spectrum*

8.1 *Introduction.* Table VII lists the 18 permitted lines selected for the analysis. Details for the three forbidden lines are given in Table VIII. The selection includes the twelve lines studied by GMA. Additional lines were selected from a list of laboratory wavelengths by Eriksson & Isberg (1963).

8.2 *Oscillator strengths*

8.2.1 *Permitted lines.* Solarski & Wiese (1964) discuss their own and other experimental measurements of O I oscillator strengths. Doherty (1961) used

TABLE VII

O I *lines in the solar spectrum*

Transition	ΔJ	λ_{air} (Å)*	χ (eV)	log gf †	W_λ‡	log W_λ/λ‡	Remarks‡
$3s\ ^5S^0$–$3p\ ^5P$	2–3	7771·94	9·15	+0·33	77	2·00	77L, 75PPC, 79A
	2–2	7774·17	9·15	+0·19	70	1·95	70L, 66PPC, 71A
	2–1	7775·39	9·15	−0·03	52	1·83	52L, 50P, 58A
$3s\ ^3P^0$–$3p\ ^3P$	1–1	8446·76	9·52	0·00	50	1·77	50PPC, 26A
	1–2	8446·36	9·52	+0·22	74	1·94	74PPC, 66A
	1–0	8446·25	9·52	−0·47			
$3p\ ^5P$–$3d\ ^5D^0$	3–	9265·9	10·74	+0·80	31	1·53	L
	2–	9262·7	10·74	+0·65	27	1·46	L
$3p\ ^5P$–$4d\ ^5D^0$	3–	6158·18	10·74	−0·29	5·9	0·98	5·9M, 3·5PPC
	2–	6156·77	10·74	−0·44	5·4	0·94	5·4M, 5PPC
$3p\ ^5P$–$4s\ ^5S^0$	3–2	11302·38	10·74	+0·03	14	1·09	L
$3p\ ^5P$–$5s\ ^5S^0$	3–2	6455·98	10·74	−0·96	2:	0·49	PPC
$3p\ ^5P$–$6s\ ^5S^0$	3–2	5436·86	10·74	−1·44	1:	0·26	PPC
$3p\ ^3P$–$4d\ ^3D^0$	1–	7001·92	10·99	−0·90	1·5:	0·33	PPC
$3p\ ^3P$–$4s\ ^3S^0$	2–1	13164·90	10·99	+0·02	10	0·88	Mo§
	1–1	13163·89	10·99	−0·29	6	0·66	Mo
$3d\ ^5D$–$5f\ ^5F$		12464·02	12·08	+0·62	8	0·81	Mo‖
$3d\ ^3D$–$5f\ ^3F$		12570·04	12·09	+0·39	4	0·50	Mo

* From Eriksson & Isberg (1963).
† Coulomb approximation.
‡ See Table II.
§ Mo = Mohler (1955).
‖ Possibly blended with an atmospheric O_2 line.

TABLE VIII

[*O* I] *lines in the solar spectrum*

Transition	ΔJ	λ_{air} (Å)*	χ (eV)	A (s^{-1})†	log gf †	W_λ‡§	log W_λ/λ§	[O]
$2p^4\ ^3P$–$2p^4\ ^1D$	2–2	6300·304	0·00	0·00697	−9·68	4·1	0·81	−0·2
	1–2	6363·776	0·02	0·00226	−10·16	2·3:	0·56	−0·1
$2p^4\ ^1D$–$2p^4\ ^1S$	2–0	5577·339	1·97	1·74	−8·09	2·0	0·56	−0·1

* From Eriksson (1965).
† See text.
‡ W_λ from Mallia & Blackwell (1967).
§ See Table VII.

shock tube as the source. All other work—Jürgens (1954), Foster (1962), Solarsk & Wiese (1964)—has been done using a stabilized homogeneous arc. There i excellent agreement between the results of the independent investigations. Solarsk & Wiese suggest that the mean values are accurate to ±25 per cent (±0·10 i log *gf*).

Both Coulomb and Hartree–Fock–Slater radial integrals (Kelly 1964) ar available. The Coulomb approximation transition integrals were examined fo evidence of strong cancellation. The transitions listed in Table IX are not subjec to strong cancellation. Varsavsky (1958) computed the oscillator strength for th strong $3s^5S^0$–$3p^5P$ multiplet. Some results for other theoretical methods are liste by GMA, and by Solarski & Wiese.

TABLE IX

gf values for O I multiplets

Transition array	Multiplet	λ (Å)	log *gf* *						
			J	SW	D	CA	K	V	NBS
$3s$–$3p$	$^5S^0$–^5P	7774	+0·70	+0·64	+0·62	+0·67	+0·72	+0·77	+0·6
	$^3S^0$–^3P	8446		+0·40	+0·38	+0·48	+0·49		+0·4
$3p$–$4s$	^5P–$^5S^0$	11302				+0·36	+0·47		+0·4
	^3P–$^3S^0$	13160				+0·19	+0·18		+0·1
$3p$–$5s$	^5P–$^5S^0$	6455	−0·63	−0·63		−0·63	−0·71		−0·6
	^3P–$^3S^0$	7254†	−0·73			−0·84	−0·98		−0·8
					F				
$3p$–$6s$	^5P–$^5S^0$	5436	−1·13		−1·25		−1·28		−1·1
	^3P–$^3S^0$	6043†	−1·40				−1·53		−1·4
$3p$–$3d$	^5P–$^5D^0$	9265				+1·13	+1·13		+1·1
$3p$–$4d$	^5P–$^5D^0$	6157	−0·02	+0·02		+0·04	−0·05		0··
	^3P–$^3D^0$	7002	−0·56			−0·42	−0·33		−0·
$3d$–$5f$	$^5D^0$–^5F	12474				+0·62	+0·61		—
	$^3D^0$–^3F	12570				+0·39	+0·38		—

* J = Jürgens (1954), CA = Coulomb approximation, SW = Solarski, Wiese (196 K = Kelly (1964), D = Doherty (1961), V = Varsavsky (1958), F = Foster (19 NBS = Wiese, Smith, Glennon (1966).

† Not listed in Table VII.

The experimental, theoretical and the NBS recommended oscillator stren are compared in Table IX. The NBS recommendations, which are an averag experimental and theoretical results, differ by less than 15 per cent from coulomb approximation results.

8.2.2 *Forbidden lines.* The [O I] lines of the multiplet $2p^4\ ^3P$–$2p^4\ ^1D$ magnetic dipole transitions. The theoretical transition probabilities for these should be accurate because no estimate of the quadrupole integral is requ Results obtained in a recent revision of forbidden line transition probabilitie adopted (Warner 1967), see Table VIII. These results differ by less than 5 per

from earlier values given by Garstang (1956). Their accuracy is put at ±10 per cent.

The [O I] line $2p^4\ ^1D_2$–$2p^4\ ^1S_0$ λ5577 is an electric quadrupole transition. Garstang (1956) computed the quadrupole integral from self-consistent field wave functions, and obtained $A = 1{\cdot}28\ s^{-1}$. Unfortunately, it is difficult to assess the accuracy of this result; Garstang suggests ±20 per cent.

No laboratory measurements of [O I] absolute transition probabilities are available. Le Blanc, Oldenburg & Carleton (1966) measured the ratio of transition probabilities for λ5577 and λ2972, which have a common upper level:

$$A(\lambda 5577)/A(\lambda 2972) = 22 \pm 2.$$

λ2972 is a magnetic dipole transition so that the theoretical transition probability can be considered well determined: $A = 0{\cdot}079\ s^{-1}$ (Warner 1967). Combining this latter value and the measured ratio a semi-experimental transition probability for λ5577 is obtained:

$A(\lambda 5577) = 1{\cdot}74 \pm 0{\cdot}15\ s^{-1}$. This value is preferred to the theoretical calculation by Garstang.

Attempts have been made to determine the radiative lifetimes of the $2p^4\ ^1D$ and $2P^4\ ^1S$ levels by observing the [O I] lines in aurorae. Unfortunately, the interpretation of the observed lifetimes is not unambiguous. The rates for collisional excitation and de-excitation cannot be precisely estimated. Therefore, it is necessary either to introduce the assumption that collisional effects are negligible or to guess values for the collisional cross-sections. In neither case are the derived radiative lifetimes likely to be reliable. In their compilation, Wiese, Smith & Glennon (1966) adopt a straight mean of auroral and theoretical values. This procedure accounts for part of the difference between our adopted and the recommended transition probabilities.

8.3 *The oxygen abundance.* For the discussion on the oxygen abundance the line lists will be split into three groups: strong permitted lines, weak permitted lines and the forbidden lines.

8.3.1 *Strong O I lines.* Three multiplets fall within this group: $3s^5S^0$–$3p^5P$, $3s^3S^0$–$3p^3P$, and $3p^5P$–$3d^5D^0$. The present analysis is incomplete for the latter two multiplets because the computer program was not designed to treat blended lines. However, by assuming that the components of a blend are either exactly coincident or completely separated, upper and lower limits for the abundance are obtained.

For line broadening calculations, the damping constants for $3s\ ^5S^0$–$3p\ ^5P$ were taken from Faulkner & Mugglestone (1962). For the other multiplets the appropriate parameters—Γ_{rad}, $\overline{R^2}$, $\Delta\nu/E^2$—were calculated from standard formulae, see Table X.

With theoretical (Coulomb approximation plus LS line strengths) oscillator strengths the abundance corrections listed in Table X were obtained.

There is a marked variation in the abundance correction [O]. The difference between the two strongest multiplets is especially disquieting. This difference is increased slightly when the experimental oscillator strengths are adopted. Since the lines are of a similar wavelength and strength the difference is too large to be attributed to errors in either the damping constants or the model atmosphere,

TABLE X

Strong O I lines

Transition	λ_{air} (Å)	$10^{-7}\,\Gamma_{rad}$	$10^{-12}\,\Delta\nu/E^2$	$\overline{R_u^2}/a_0^2$	$\overline{R_l^2}/a_0^2$	[O]
$3s\ ^5S^0$–$3p\ ^5P$	7771·94	34	0·89	44	25	−0·17
	7774·17					−0·14
	7775·39					−0·18
$3s\ ^3S^0$–$3p\ ^3P$	8446·76	30	2·4	54	29	+0·01
	8446·36					−0·11 < [O] < +0·08
	8446·25					
$3p\ ^5P$–$3d\ ^5D^0$	9265·9	40	17	120	44	[O] < −0·20
	9262·7					[O] < −0·16

see Section 14.2. Therefore, both the theoretical and experimental oscillator strengths must be considered as the source of this variation. Systematic errors in the experimental results are not unlikely. The presence of weak intercombination lines in laboratory spectra is indicative of departures from LS-coupling. Eriksson & Isberg (1963) identified intercombination lines in the solar spectrum. From the equivalent widths of these lines we estimate that their multiplet strength is less than one per cent of that for the strong transitions. Much larger effects are required to explain the observed discrepancies.

In the following section it is shown that the multiplet $3p^3P^0$–$4s^3S$ is weaker by a factor two than predicted on the basis of the theoretical oscillator strengths. The multiplet $3p^5P^0$–$4s^5P$ is not noticeably weaker. Further of the corresponding transitions in the $3p$–$3s$ array λ8446 ($^3P^0$–^3S) is stronger than λ7774 ($^5P^0$–^5P). This evidence suggests that for transitions involving the $3p\ ^3P^0$ levels the theoretical oscillator strengths are unreliable; this can probably be attributable to departures from LS coupling. In view of this suggestion the abundance correction is obtained from the λ7774 triplet, that is [O] = −0·17. The uncertainty is difficult to estimate—perhaps ±0·05.

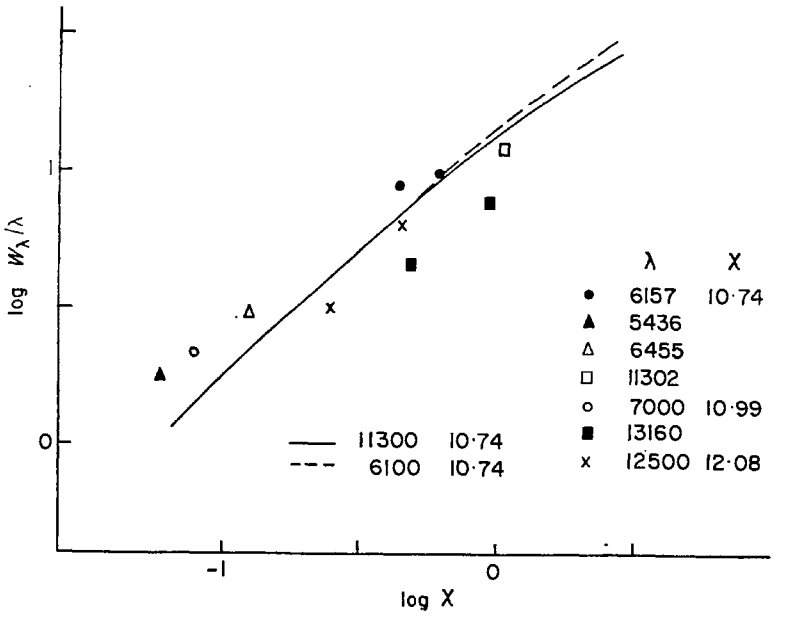

FIG. 7. *A composite curve of growth for weak permitted O I lines. The solid line corresponds to* [O] = −0·07.

8.3.2 *Weak O I lines.* The composite curve of growth for this group of ten lines is given in Fig. 7. Four lines are very weak (log $W_\lambda/\lambda < 0\cdot5$) and should be given low weight. The multiplet $3p\ ^3P^0$–$4s\ ^3S$ at λ13160 Å provides an abundance a factor two smaller than that from the other lines. If this multiplet and the four weakest lines are excluded, the four remaining lines give [O] = $-0\cdot07\pm0\cdot05$ with the theoretical oscillator strengths. With experimental oscillator strengths [O] is increased to $+0\cdot00$ or $+0\cdot05$.

8.3.3 *[O I] lines.* The Oxford photoelectric spectrometer (Blackwell, Petford & Mallia 1967), was used to re-observe the weak [O I] lines. A noise level of $\pm0\cdot02$ per cent was achieved. This is a considerable improvement on previous spectra for these lines. The accuracy of the equivalent widths is high and limited only by the uncertainty in the positioning of the continuum level and by the possibility of contamination by unidentified lines. The equivalent widths (Mallia & Blackwell 1967) are listed in Table VIII. Earlier observations are discussed by Swings (1966).

The resultant abundance corrections are listed in the final column of Table VIII. The weighted mean is $-0\cdot20\pm0\cdot05$, where weights of four, two and one were assigned to λ6300, λ5577, and λ6363, respectively on the basis of the uncertainty in their equivalent widths.

8.3.4 *Discussion.* In the determination of the oxygen abundance GMA gave the greater weight to the λ7774 triplet. In the present paper an attempt has been made to justify the exclusion of λ8446 from the abundance determination. Since line damping is included in the present calculations the abundance for the λ7774 triplet is less than the GMA result. The [O I] lines also give a smaller abundance than GMA obtained for these lines. The reduction is attributable to a change in the equivalent widths and to a lesser extent in the transition probabilities. The abundances from λ7774 triplet and the [O I] lines are in good agreement. The weak O I lines indicate a larger abundance and this problem is discussed in a later section.

Molecular Spectra

9.1 *Introduction.* Previous abundance determinations from molecular spectra have been subject to considerable uncertainty, owing to a lack of reliable oscillator strengths and, in some cases ill-determined dissociation energies. Substantial improvements in both directions have been achieved in recent years. Therefore, a re-examination of molecular spectra is undertaken.

Five bands are discussed in the following sections: C_2 Swan Band, red and violet CN bands, CO vibration–rotation overtone bands, and the $A^2\Delta$–$X^2\Pi$ CH band.

9.2 *The line oscillator strength.* A certain degree of confusion exists in the literature concerning the definitions of line, band and electronic oscillator strengths. Throughout this paper the definitions discussed by Schadee (1967) are adopted. A similar but not exactly equivalent discussion is that by Tatum (1967).

Following Schadee, the line oscillator strength for the transition between the lower level (n'', v'', J'') and the upper level (n', v', J') is written

$$f_{J'J''} = \frac{8\pi^2 m_e}{2he^2\lambda_{J'J''}} \cdot \frac{\Sigma|R_e^{v'v''}|^2}{(2-\delta_{0,\Lambda''})(2S''+1)} \cdot \frac{S_{J''J'}}{(2J''+1)} = \frac{\lambda_{v'v''}}{\lambda_{J'J''}} f_{v'v''} \frac{S_{J''J'}}{2J''+1}$$

The standard notation of molecular spectroscopy is adopted. The Hönl–London factors $S_{J''J'}$ are normalized according to the sum rule (Schadee 1967).

$$\sum_{\Sigma'\Sigma''} \sum_{J'} S_{J''J'} = (2S''+1)(2J''+1).$$

In the case of Λ degeneracy the oscillator strength is an average for the Λ-doublet.

In the literature the electronic oscillator strength is commonly used. Definitions of this quantity differ slightly. In adopting results culled from the literature care has been taken to ensure that the quoted oscillator strength is compatible with the above definition of the band oscillator strength $f_{v'v''}$.

10. *The C_2 Swan Band ($A\ ^3\Pi_g$–$X'\ ^3\Pi_u$)*

10.1 *Introduction.* The identifications for the (0, 0) Swan band are well established. Unfortunately the several sets of equivalent width observations are not in complete agreement. Schadee (1964) discussed the equivalent widths published in the Preliminary Photometric Catalogue. Laborde (1961) measured equivalent widths on plates taken with the Meudon spectrograph. These latter values are approximately a factor 1·5 larger than the Preliminary Photometric Catalogue measurements. In an attempt to reduce this discrepancy Mallia (1967) kindly undertook the re-observation of selected C_2 lines with the Oxford photoelectric spectrometer. His results are given in Table XI, and compared in Fig. 8 on the standard log $W_{N''}/S_{N''}$ vs $N''(N''+1)$ plot with the mean lines obtained from Schadee's and Laborde's equivalent widths. An appreciable scatter remains, which is probably attributable to unidentified blends. For this investigation averaged equivalent widths are adopted (see broken line in Fig. 8). The uncertainty in log $W_{N''}/S_{N''}$ is about $\pm 0{\cdot}10$ but the equivalent uncertainty in the carbon abundance is only $\pm 0{\cdot}05$.

TABLE XI

C_2 Swan Band equivalent widths

Line*	λ (Å)	W_λ (mÅ)†		
		M	PPC	LAB
P_1+P_2 (27)	5159·464	13·9	18	
P_3 (27)	5159·605	10·1		
P_1+P_2 (28)	5158·525	17·4	17	
P_3 (28)	5258·664	5·9		
P_1+P_2 (44)	5135·583	21·4	16	12·6
P_3 (44)	5135·711			8·1
R_1 (15)	5136·274	11·4	11	11·0
R_2 (15)	5136·456	6·9	8	6·9
R_1+R_2 (44)	5063·164	12·1	16·5	14·7
R_3 (44)	5063·290	5·7		10·3

* See Schadee (1964).

† M = Mallia (1967), LAB = Laborde (1961), PPC = Preliminary Photometric Catalogue.

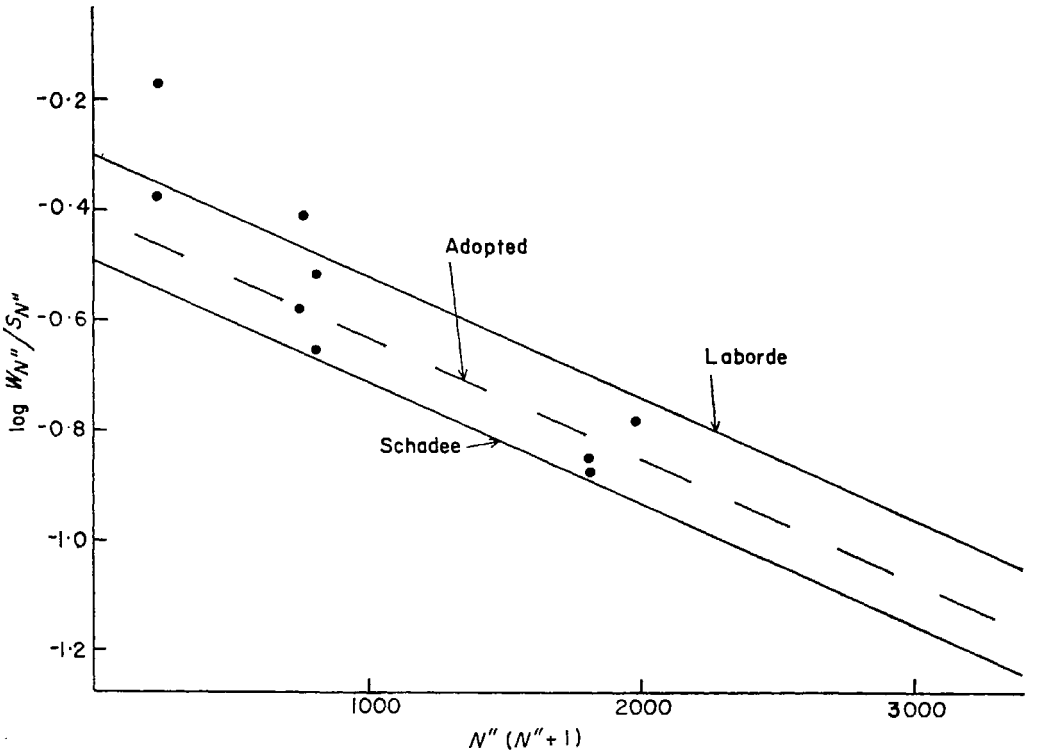

FIG. 8. *The C_2 (0, 0) Swan Band: a plot of log $W_{N''}/S_{N''}$ vs $N''(N''+1)$. The solid circles denote the lines reobserved by Mallia* (1967). *The adopted straight line, which is shown by the broken line is compared with earlier results by Laborde* (1961) *and by Schadee* (1964).

10.2. *Dissociation energy.* Previous attempts to derive the carbon abundance from the Swan bands foundered because the dissociation energy of C_2 was ill-determined. The analysis was frequently reversed to obtain an astrophysical estimate for the dissociation energy. Moreover, the identification of the ground state and, therefore, the excitation potential of the $X'\ ^3\Pi$ level was in doubt.

Ballik & Ramsay (1959, 1963) established that the $^1\Sigma_g^+$ state, which lies 610 cm^{-1} or 0·075 eV below the $X'\ ^3\Pi_u$ state, must be the ground state. Brewer, Hicks & Krikorian (1962) summarized measurements of the dissociation energy and recommended the value $D_0(C_2) = 6{\cdot}25 \pm 0{\cdot}2$ eV. This value is adopted.

10.3. *Band oscillator strength, f_{00}.* Eight measurements of the (0, 0) band oscillator strength are summarized in Table XII. The results from four independent shock-tube experiments are in agreement to within the stated errors. Such inter-agreement suggests that a large systematic error is unlikely. A 'best' value $f_{00} = 0{\cdot}020 \pm 0{\cdot}005$ is adopted.

Two of the measurements listed in Table XII are not in good agreement with the adopted value. Fairbairn (1966) discusses Hagen's experiments and states that her data show a marked scatter; one set gave $f_{00} = 0{\cdot}043$. It appears probable that the uncertainty of her result was grossly underestimated. The lifetime measurement, Jeunehomme & Schwenker (1965) is of apparently high accuracy but is in marked disagreement with the shock-tube results. Fairbairn criticized several aspects of this work. It is clear from this that a more detailed experimental investigation should be undertaken before it can be safely asserted that the

TABLE XII

Swan Band oscillator strengths

f_{00}	Method	Reference
$0{\cdot}005 \pm 0{\cdot}003$	King furnace	Hagen (1963)
$0{\cdot}019$*	King furnace	Hicks (1957), revised by Fairbairn (1966)
$0{\cdot}00433 \pm 0{\cdot}00012$	Laser excitation: lifetime measurement	Jeunehomme & Schwenker (1965)
$0{\cdot}016 \pm 0{\cdot}006$	Shock tube	Sviridov *et al.* (1965)
$0{\cdot}019 \pm 0{\cdot}004$	Shock tube	Sviridov *et al.* (1966a)
$0{\cdot}022 \pm 0{\cdot}022$	Shock tube	Sviridov *et al.* (1966b)
$0{\cdot}024 \pm 0{\cdot}009$	Shock tube	Fairbairn (1966)
$0{\cdot}020 \pm 0{\cdot}009$	Shock tube	Harrington, Modica & Libby (1966)

* Uncertain to within a factor 2 (Clementi 1960).

measured lifetime is equivalent to the radiative lifetime of the $A\ ^3\Pi$ level. It is to be hoped that this will be done.

Theoretical estimates of the electronic transition moment $|R_e^{v'v''}|^2$ for the C_2 Swan transition will not be discussed because the precision attainable in theoretical calculations is inferior to that in shock tube experiments.

10.4 *Carbon abundance.* With the adopted model atmosphere, the GMA abundance, a dissociation energy of 6·25 eV, $f_{00} = 0{\cdot}020$, and with the formation of CO taken into account, the predicted equivalent widths are about a factor two larger than the observed values. To within the observational uncertainty, the variation of equivalent width with rotational quantum number is reproduced in the calculations. The carbon abundance is

$$\log A_C = -3{\cdot}40 \pm 0{\cdot}20 \text{ or } [C] = -0{\cdot}12 \pm 0{\cdot}20$$

for [O] = 0·00. The uncertainty is apportioned as follows: $\pm 0{\cdot}10$ owing to error in D_0, $\pm 0{\cdot}05$ from f_{00}, and $\pm 0{\cdot}05$ from the equivalent width observations. Additional errors resulting from model atmosphere uncertainties are discussed in Section 14·2.

The carbon abundance is slightly dependent on the assumed oxygen abundance: a change of $\pm 0{\cdot}2$ in $\log A_O$ produces a change of $\pm 0{\cdot}03$ in $\log A_C$. The locus of the solution for [C] is given in Fig. 12.

11. *The CN red and violet systems*

11.1 *Introduction.* Cowley (1964) discussed the CN violet system($B^2\Sigma^+$–$X^2\Sigma^+$). The equivalent widths of selected lines were measured on McMath–Hulbert tracings. His equivalent widths are rediscussed in terms of the new model atmosphere and revised values for the dissociation energy and band oscillator strength.

Although the CN Red system ($A\ ^2\Pi$–$X^2\Sigma^+$) is an established feature of the infrared solar spectrum, no detailed discussion of identifications and equivalent widths is available for even the strongest two bands—the (0, 0) and (1, 0) vibrational bands. Rigutti (1962) working from a list of laboratory wavelengths for 569 lines in the (0, 0) and (1, 0) bands identified only 38 in the solar spectrum.

The present discussion is restricted to the (0, 0) band. The (1, 0) and weaker bands are discussed elsewhere (Lambert 1967a). With the wavelengths given by Davis & Phillips (1963) and the excellent Liège Atlas 50 unblended lines were identified and measured. An additional 50 lines were identified by extrapolation of the laboratory wavelengths to higher rotational quantum numbers. The identifications, wavelengths and equivalent widths for the (0, 0) band are given in Table XIII.

Solar identifications for the weaker (2, 0) and (3, 1) bands were proposed by Rigutti & Drago-Chiuderi (1963). The equivalent widths were discussed by Rigutti & Poletto (1965). These bands are not included in the present discussion because of the considerable scatter in the equivalent widths.

11.2 *Dissociation energy.* The controversy concerning the dissociation energy of CN was resolved as a result of the experimental work by Berkowitz (1962) and by Knight & Rink (1962). On the basis of these experiments Wilkinson (1963) recommends the value $D_0 = 7{\cdot}5$ eV, which is adopted for the present investigation.

An earlier spectroscopic investigation gave $D_0 = 8{\cdot}22$ eV (Carroll 1956). Tsuji (1964) points out that the introduction of a lower value of $7{\cdot}5$ eV introduces some apparent inconsistencies into the dissociation energies of the molcules HCN and C_2N_2. Such problems lie outside the scope of this paper. However, it is later shown that when the analysis is reversed the lower value of D_0 is to be preferred, see Section 14.1.

11.3 *Band oscillator strengths*

11.3.1 *CN violet system, f_{00}.* Bennett & Dalby (1962) measured the radiative lifetime of the $B^2\Sigma^+$ state. The CN bands were excited by pulsed electron bombardment of HCN at the lower pressure. The possibility of collisional de-excitation (quenching collisions) was examined and rejected. The (0, 0) band oscillator strength is $f_{00} = 0{\cdot}025 \pm 0{\cdot}003$, where the Franck–Condon factor $q_{00} = 0{\cdot}918$ (Spindler 1965), was used to convert the published electronic oscillator strength (f_{el}) to f_{00}.

Sobolev and colleagues made absolute intensity measurements of CN emission from a shock tube (Kundryatsev *et al.* 1963). Their result on conversion to a band oscillator strength gives $f_{00} = 0{\cdot}027 \pm 0{\cdot}004$.

Fairbairn (1964) also from a shock-tube experiment measured the transition probability. The band oscillator strength appropriate to $D_0 = 7{\cdot}55$ eV is $f_{00} = 0{\cdot}035 \pm 0{\cdot}017$.

Reis (1965) measured the CN emission from the shock layer about a hypervelocity projectile. For $D_0 = 7{\cdot}55$ eV, his result is $f_{00} = 0{\cdot}10 \pm 0{\cdot}05$.

The band oscillator strength $f_{00} = 0{\cdot}026 \pm 0{\cdot}003$ is adopted for the present investigation.

11.3.2 *CN red system.* Jeunehomme (1965) measured the radiative lifetime for the vibrational levels $v' = 1$ to $v' = 9$ in the $A\ ^2\Pi$ state. CN radicals were excited in an electrode-less discharge in acetonitrile. Collisional de-excitation was eliminated by running the discharge at a low pressure and extrapolating the observed lifetimes to zero pressure. The band oscillator strength was given as $f_{00} = (3{\cdot}4 \pm 0{\cdot}3) \times 10^{-3}$. This result was based upon calculations made with

TABLE XIII

The (0, 0) band of the CN red system: selected lines

Q_1 branch			Q_2 branch		
N''	λ	W_λ (mÅ)	N''	λ	W_λ
6	10998·741	7·8	4	10945·141	4·2
7	11000·678	8·9	5	10948·848	5·9
10	11009·602	13	14	10998·080	13
15	11034·871	17	17	11021·379	13
23	11101·271	20	29	11153·388	20
33	11228·822	21	37	11278·701	21
41	11367·643	22	46	11458·75	15
42	11387·45	19	48	11504·70	16
43	11407·75	20	49	11528·60	19
44	11428·60	15	50	11552·95	16
45	11449·95	18	52	11603·55	12
52	11615·80	14	53	11629·90	13
53	11641·80	16	55	11684·05	13
55	11695·80	13	56	11712·00	12
56	11723·65	15	57	11740·70	11
59	11811·15	13	59	11799·90	10·5
60	11841·70	12	60	11830·50	8·3
62	11904·70	8·8	62	11893·60	8·6
63	11937·15	8·2	63	11926·20	7·8
			64	11959·35	9·0
			65	11993·45	6·9

R_1 branch			R_2 branch		
4	10974·573	3·3	10	10928·405	9·0
6	10968·730	3·8	12	10932·055	8·5
15	10968·354	11	13	10934·413	7·2
16	10970·827	8·3	27	11010·751	8·8
21	10990·337	11	28	11019·455	11·5
22	10995·698	10·5	33	11069·663	11
23	11001·495	10·3	35	11092·997	10
25	11014·578	13	41	11174·391	10
26	11021·789	9·7	45	11238·518	9·5
31	11065·159	13	52	11370·650	7·3
34	11096·960	13	53	11391·75	7·0
40	11173·768	9·0	59	11529·70	9·5
48	11304·568	8·3	62	11606·45	5·2
51	11362·293	7·2			
54	11425·10	6·5			
60	11565·85	5·5			
62	11617·55	5·5			
63	11644·25	4·0			
64	11671·75	5·0			
66	11728·40	4·5			
68	11787·70	3·5			

TABLE XIII (*continued*)

P_1 branch			P_2 branch		
25	11229·619	9·9	12	11033·217	6·5
28	11279·131	11	13	11044·087	6·2
34	11392·75	13	15	11066·995	6·5
38	11479·40	12	18	11104·517	9·5
40	11526·10	9·1	23	11175·893	11
44	11626·65	10	25	11207·665	8·8
47	11708·30	9·0	34	11375·104	11
49	11765·95	6·1	36	11418·10	12
52	11857·20	8·5	39	11486·50	11
54	11921·45	5·6	42	11559·90	8·1
			43	11585·55	7·2
			46	11666·10	9·2
			48	11722·75	9·5
			50	11781·95	7·0
			52	11843·75	5·8
			53	11875·70	8·8

Morse potentials. A re-analysis of the lifetime data using the more realistic RKR potentials gives a slight reduction: $f_{00} = (3\cdot3 \pm 0\cdot3) \times 10^{-3}$ (Lambert 1967a). This value is adopted for the present analysis.

11.4 *Abundance analysis*

11.4.1 *CN violet system.* Curves of growth for the CN (0, 0) band, which consists of close doublets, were computed by Cowley (1964). The present model and the Müller–Mutschlechner model used by Cowley are very similar and significant differences in the shape of the curves of growth are not anticipated. The Cowley curves are adopted and fitted to a recomputed linear portion derived from the present model.

With $f_{00} = 0\cdot026$, $D_0 = 7\cdot5$ eV and [O] = 0·00, a best fit to the observed equivalent widths is obtained for $\log A_C A_N = -7\cdot48$ or [C]+[N] = $-0\cdot18 \pm 0\cdot15$. The result is slightly dependent on the assumed oxygen abundance (see Section 10.4 above). The principal contribution to the estimated error arises from the uncertainty in the dissociation energy.

It is well known that an unidentified source of continuous opacity is present for $\lambda < 5000$ Å. This was not taken into account in the calculations. Calculations reported by Cowley suggest that the effect of inclusion of the opacity is to increase the correction [C]+[N] by about +0·05. Line damping was assumed to be zero (Cowley 1966) and the introduction of damping introduces a correction of perhaps −0·05 to −0·10.

Cowley pointed out that for values of f_{00} and D_0 almost identical to the present adopted values the predicted equivalent widths based on the GMA abundances were close to the observed values. This conclusion, which is contradicted by the present results, appears to be due to incorrect normalization of the Höln–London factors.

11.4.2 *CN red system.* The observed and predicted equivalent widths for the (0, 0) band are compared in Fig. 9. The optimum fit corresponds to the abundances:

$$\log A_C A_N = -7\cdot58 \text{ or } [C]+[N] = -0\cdot28 \pm 0\cdot15$$

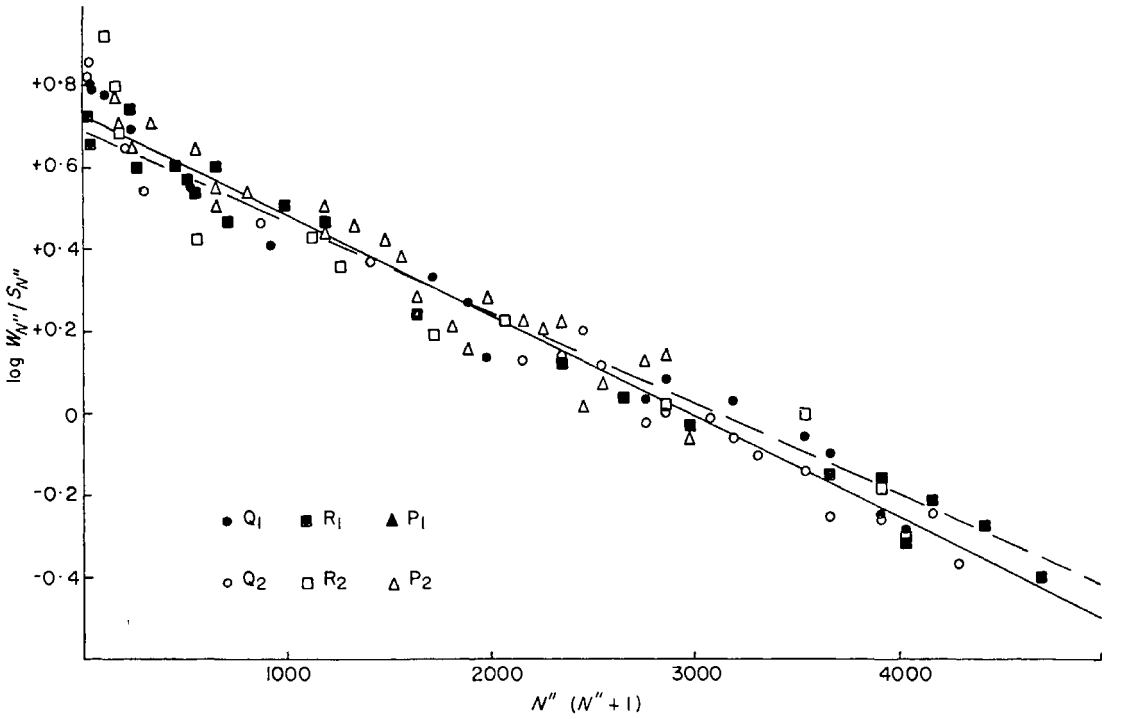

FIG. 9. *The* (o, o) *band of the CN red system: a plot of log* $W_{N''}/S_{N''}$ *vs* $N''(N''+1)$. *The solid line shows the least-squares fit to the observations. The broken line gives the model atmosphere prediction which provides the optimum fit to the observations. The small difference in slope between the solid and broken lines is less than the probable error of the least-squares solution.*

The predictions are in good agreement with the observations for the observed range of rotational quantum number, see Fig. 9.

The independent solutions for the red and violet bands are in very good agreement. The difference of about 25 per cent is attributable to oscillator strength uncertainties. The [C]+[N] loci are plotted in Fig. 12.

12. *CO vibration–rotation first overtone bands*

12.1 *Introduction.* The first overtone bands of the carbon monoxide vibration–rotation spectrum at 23 000–24 000 Å were first identified in the solar spectrum by Goldberg and his colleagues (1952). Newkirk (1957) discussed their strength and centre–limb variation. His equivalent widths for the centre of the disk are rediscussed.

12.2 *Dissociation energy.* The dissociation energy of CO has been well determined: $D_0 = 11{\cdot}09$ eV (Chupka & Ingram 1955, Herzberg 1957, Wilkinson 1963). The uncertainty in D_0 is unlikely to exceed $\pm 0{\cdot}02$ eV.

12.3 *Line oscillator strengths.* The standard notation for vibration–rotation transitions differs from that for electronic transitions. Following Young & Eachus (1966) the line oscillator strength for the transition $(v'', J'')\rightarrow(v' = v''+n, J')$ is written as

$$f_{v''J''v'J'} = \frac{8\pi^2 m_e c\nu}{3e^2h} \cdot \frac{|m|}{2J''+1} \cdot |R_{v''}^{v''+n}|^2 F_{v''}^{v''+n}(m)$$

where ν = the wave number for the transition;
m = the rotational index: $m = J''+1$ for the R branch,
$= -J'$ for the P branch;
$R_{v''}^{v''+n}$ = the vibrational matrix element;
$F_{v''}^{v''+n}(m)$ = the Herman–Wallis factor;
n = 2 for first-overtone bands.

Young & Eachus considered all the available data on integrated absorption coefficients for the fundamental, first and second overtone bands. Their values for $|R_{v''}^{v''+n}|^2$ and $F_{v''}^{v''+n}(m)$ are adopted. The accuracy of the line oscillator strength is about 10 per cent.

12.4 *Abundance analysis.* The locus of the solution for [C]+[O] is plotted in Fig. 12; for [O] = 0, [C] = − 0·40. The uncertainty in [C]+[O] is probably about ±0·10.

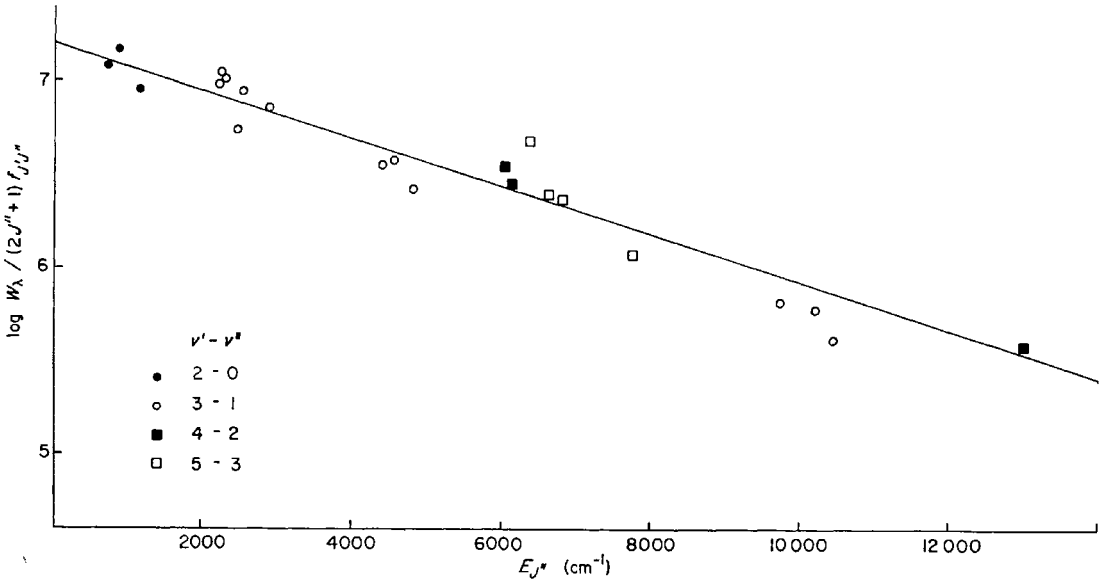

FIG. 10. *The CO first overtone bands of CO: a plot of log* $W_\lambda/(2J''+1)f_{J''J'}$ *vs* $E_{J''}$. *The solid line shows the model atmosphere prediction which provides the optimum fit to the observations.*

The observations and the predictions for the revised abundances are compared in Fig. 10. This is a plot of log $W_\lambda/(2J''+1)f_{J''J'}$ vs $E_{J''}$ the excitation potential (in cm^{-1}) of the lower level (v'', J''). The agreement is good. Unfortunately, Newkirk's observations are too limited to investigate possible variations between bands.

13. *The CH A* $^2\Delta$–*X* $^2\Pi$ *band*

13.1 *Introduction.* The *A* $^2\Delta$–*X* $^2\Pi$ system at λ4300 Å is the stronger of the CH systems appearing in the solar spectrum. Moore & Broida (1959) discussed the identification of CH lines. This analysis is confined to the *Q* and *R* branches of the (0, 0) band. 67 lines were selected with the identification CH. Approximately 15 lines were rejected because the observed equivalent width appeared either too strong or too weak by a factor of more than two. Equivalent widths for the lines were extracted from The Preliminary Photometric Catalogue.

13.2 *Dissociation energy.* The standard determination of the CH dissociation energy is that by Herzberg (1950, 1957) which is based on spectroscopic observations of predissociation by Shidei (1936): Herzberg found $D_0 = 3{\cdot}47$ eV. From a study of CH radicals in thermal equilibrium in a carbon furnace with H_2 gas Brewer & Kester (1964) obtained $D_0 = 3{\cdot}5 \pm 0{\cdot}2$ eV. The predissociation method is the more accurate and $D_0 = 3{\cdot}47$ is adopted.

13.3 *Band oscillator strength,* f_{00}. Bennett & Dalby (1960) applied their technique of pulsed electron bombardment with methane (CH_4) as the target gas to measure the radiative lifetime of the $A\ ^2\Delta$ state. Their result converted to a band oscillator strength is $f_{00} = (4{\cdot}9 \pm 0{\cdot}5) \times 10^{-3}$, where the Franck–Condon factor $q_{00} = 0{\cdot}9996$ (Childs 1964), was adopted.

No measurements of absolute emission intensities or total absorption are reported in the literature. Experimental work quoted by Stephenson (1951) refers to the radical OH not CH. Using simple wave-functions Stephenson calculated $f_{00} = 8 \times 10^{-3}$ but the accuracy of this result is uncertain.

Hönl–London factors for the $^2\Delta$–$^2\Pi$ transition of CH were computed by Arpigny (1966).

13.4 *Abundance analysis.* The linear portion of the curve of growth was computed by the weighting function method. Results presented by Baschek (1963) enabled the shoulder of the curve of growth to be reconstructed. It was assumed that the curve of growth would have the same shape for the adopted model. Baschek's curve was then fitted to the recomputed linear portion. A similar procedure gave satisfactory results for the CN violet system.

The curve of growth (log W_λ vs log $S_{J''J'} - (\chi_{exc} - 0{\cdot}211)$) is given in Fig. 11 The displacement of the theoretical curve, which is necessary to fit the observations, gives the abundance

$$\log A_C = -3{\cdot}68 \text{ or } [C] = -0{\cdot}40 \pm 0{\cdot}10 \text{ for } [O] = 0{\cdot}00.$$

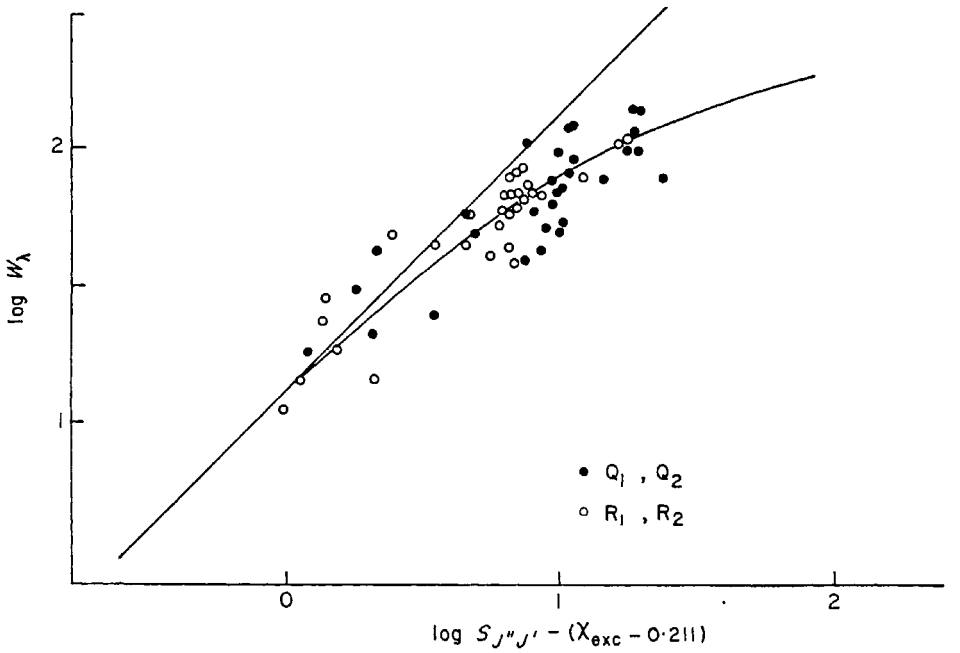

FIG. 11. *A curve of growth for lines from the Q and R branches of the* (0, 0) *band of the* $A^2\Delta$–$X^2\Pi$ *system of CH.*

This carbon abundance is markedly less than that obtained from the C I spectrum and other molecules, see Fig. 12.

14.1 *Discussion*

In preceding sections no attempt was made to compare abundances derived from molecular and atomic spectra. The results are summarized in plots of [O] vs [C] and [N] vs [C], see Figs 12(a)–(b).

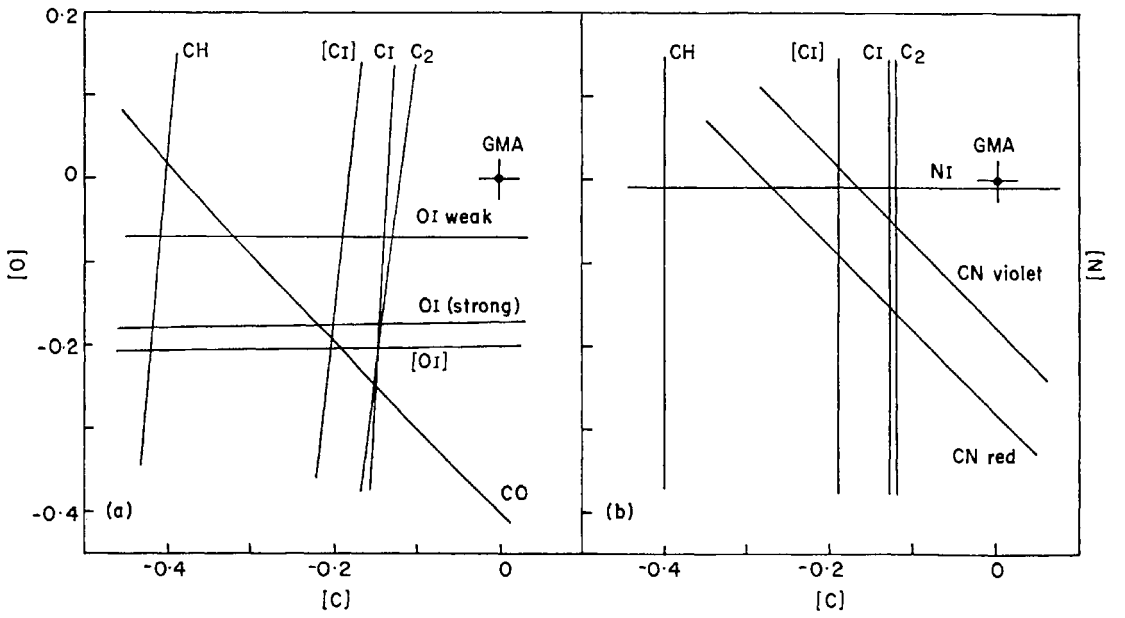

FIG. 12. *The abundance determinations from atomic and molecular spectra displayed in plots of* (a) [*O*] *vs* [*C*], *and* (b) [*N*] *vs* [*C*].

The excellent agreement between the molecular and atomic spectra must be noted: the CH ($A\ ^2\Delta$–$X\ ^2\Pi$) band is the one exception. Before introducing a discussion of the effect on the abundances of model atmosphere errors, some comments on particular aspects of Figs 12(a), (b) will be presented.

First, the possible reasons for the CH discrepancy will be examined. The predissociation observations, which are confirmed by the recent thermal measurements, establish an accurate value for the dissociation energy. In view of this the oscillator strength must be assumed to be in error. If quenching collisions were effective, the resultant oscillator strength, which is deduced from the measured lifetime for the upper state, would be too large. This effect is of the correct sense to explain the discrepancy. However Bennett & Dalby (1960) examined this possibility and concluded that such collisions were ineffective. It is to be hoped that further observations of the oscillator strength will be undertaken. The revised carbon abundance (see Section 15) and the CH observations result in an empirical oscillator strength for the band of $f_{00} = (2{\cdot}8 \pm 0{\cdot}8) \times 10^{-3}$.

In Section 10.3 it was noted that the apparently accurate lifetime determination of the Swan band oscillator strength by Jeunehomme & Schwenker (1965) was not in good agreement with results obtained from shock tube studies. The lifetime oscillator strength results in a carbon abundance given by [C] = $+0{\cdot}05 \pm 0{\cdot}15$ for [O] = 0·00. From Figs 12(a), (b) it is clear that the solution [C] = $-0{\cdot}15$ is indicated. The difference in these results does suggest that the lifetime oscillator

strength is too small by a rather larger factor. Clearly, if a more accurate determination of the C_2 dissociation energy were available, this method could provide a better test.

The CN systems give abundances in good agreement with other results. This result confirms the choice of dissociation energy. A high value $D_0 = 8{\cdot}2$ eV (see Section 11.2) is not consistent with the abundance results; it corresponds to a shift of the CN solution by $-0{\cdot}65$ in [N].

Of the results from atomic spectra, one feature deserves further comment at this stage. The weak lines of high excitation potential in the O I and N I spectra suggest a higher value for the abundance than other results. For O I this result is evident from Fig. 12(a). For N I the abundance obtained with the theoretical oscillator strengths is plotted. The discrepancy appears only if the experimental oscillator strengths are adopted. This observation ought to be examined further. In the discussion on the model atmosphere, the importance of determining the temperature distribution at large optical depths is outlined.

Especially pleasing is the good agreement in the C I and O I spectra between the strong permitted lines and the weak forbidden lines. These lines are formed in similar parts of the atmosphere and the agreement indicates that the model must be substantially correct. This is further discussed in the next sections.

14.2 *The model solar atmosphere.* Before a final assessment of the carbon, nitrogen, and oxygen abundances, the effect on the abundances of a variety of uncertainties in the model solar atmosphere will be discussed. The following topics are examined:

(a) the absolute intensity calibration of the continuous spectrum;
(b) the error in the temperature distribution $T(\tau_0)$ and the effect of granulation;
(c) the assumed metal content;
(d) the assumed helium content;
(e) the microturbulence;
(f) the continuous absorption coefficients.

14.2.1 *The absolute intensity,* I_λ (0, 0). The model solar atmosphere (Table I) was constructed to reproduce the absolute intensity measurements published by Labs & Neckel (1962, 1963). As an alternative, the model might have been normalized to the intensity scale proposed by Makarova (1964). The adjustment of the model is most readily achieved by a uniform decrease in the reciprocal temperature: $\Delta\theta = -0{\cdot}028$. As is well known, this alteration will not affect the limb darkening predictions. Qualitatively, the result of the temperature increase can be foreseen. Higher abundances are required to fit the molecular lines and lower abundances are obtained from the high excitation atomic lines. Figs 13(a), (b) show the abundance plots, which are obtained from a model atmosphere which fits the Makarova energy distribution at λ5000 Å. This diagram demonstrates the significance of the analysis of CO and CN spectra. They provide an important restraint on the model and, therefore, an abundance determination of greater accuracy. From Fig. 13(a), it will be seen that the CO spectra cannot simultaneously satisfy the separate determinations from atomic spectra. A similar conclusion is obtained from Fig. 13(b) and the CN results. Similar but smaller shifts are observed

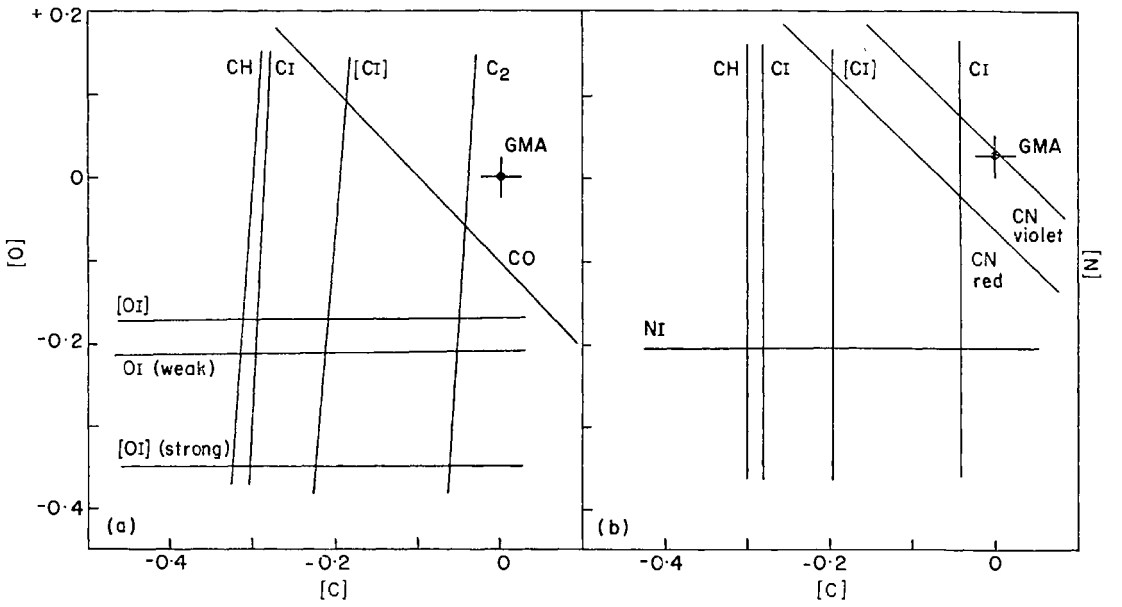

FIG. 13. *The abundance determinations from atomic and molecular spectra obtained with a model atmosphere, which was normalized to the Makarova* (1964) *absolute intensity distribution (see text):* (a) [*O*] *vs* [*C*], *and* (b) [*N*] *vs* [*C*].

for the abundances derived from the permitted and forbidden atomic lines. Such discrepancies are too large to be attributed to even the most favourable combination of errors. The conclusion must be that the Makarova energy distribution is unacceptable.

The combination of atomic and molecular spectra confirms Labs & Neckel's observations of the absolute intensity of the solar continuous spectrum. The present method provides an accuracy of about ± 4 per cent compared with the accuracy of $\pm 2{\cdot}5$ per cent quoted by Labs & Neckel.

14.2.2 *The temperature distribution and granulation.* The model solar atmosphere was constructed to fit the continuum observations for a wide range in wavelength and of disk position. The resultant temperature distribution is well defined over a wide range in $\log \tau_0$. The probable temperature errors, which were estimated by a modification of the method proposed by Thomas & Athay (1961) are: In the range

$\log \tau_0 \geqslant +0{\cdot}7$	$\Delta T_e \geqslant \pm 200°$
$+0{\cdot}3 \leqslant \log \tau_0 \leqslant +0{\cdot}7$	$\pm 50° \leqslant \Delta T_e \leqslant \pm 100°$
$-1{\cdot}5 \leqslant \log \tau_0 \leqslant +0{\cdot}3$	$\Delta T_e \leqslant \pm 50°$
$-2{\cdot}2 \leqslant \log \tau_0 \leqslant -1{\cdot}5$	$\pm 50° \leqslant \Delta T_e \leqslant \pm 100°$
$-3{\cdot}0 \leqslant \log \tau_0 \leqslant -2{\cdot}2$	$\pm 100° \leqslant \Delta T_e \leqslant \pm 200°$
$\log \tau_0 \leqslant -3{\cdot}0$	$\Delta T_e \geqslant \pm 200°$

These errors do not include possible contributions from uncertainties in the absolute intensity scale.

The forbidden lines—[C I] and [O I]—are, of course, insensitive to the small temperature changes. The weak permitted lines are of high excitation potential and are formed at large optical depths: the abundance error is $[\alpha] \approx \pm 0{\cdot}07$. The

errors in the predicted equivalent width for the strong permitted atomic lines and the molecular lines are of opposing sign and equal to about 0·05 dex.

The excellent agreement (see Fig. 12) between the solutions obtained from atomic and molecular spectra is good evidence that temperature errors are unimportant.

Finally, a brief comment should be made on the use of a homogeneous model which makes no attempt at a representation of the solar granulation. The assumption that the temperature fluctuations are independent of depth provides the simplest model for granulation. The magnitude of the temperature fluctuations can be derived from the observed granulation intensities. It can easily be shown that with the introduction of a two or three stream model, which gives the same predicted average continuum intensities as the homogeneous model, the abundances obtained from both high excitation lines ($\chi_{exc} \approx 10$ eV) and the molecular lines ($D_0 \simeq 10$ eV) will be reduced by about 0·05 dex. This reduction might account for the small abundance differences between the permitted and forbidden lines of C I and O I.

The observations of the centre–limb variation of the granulation contrast can be interpreted to show that the temperature fluctuations must have a maximum value at about $\log \tau_0 = -0{\cdot}2$ (Edmonds 1962) and, therefore, the introduction of a two or three stream model will primarily affect the abundances derived from the weak high-excitation lines, see Fig. 2. This might explain the discrepancy between the weak and strong permitted lines in O I.

14.2.3 *The metal content.* In the calculation of gas and electron pressures the abundances of the principal electron donors were taken from Lambert & Warner (1967). The change in the abundance for carbon, nitrogen, or oxygen corresponding to a uniform change in the metal abundances by factors of $\frac{1}{2}$ and 2 were calculated.

Results are as follows:

[C I], [O I], O I and C I strong lines:	$\Delta \log W_\lambda \approx \pm 0{\cdot}08$
N I, O I weak lines:	$\approx 0{\cdot}00$
molecular lines:	$\approx \pm 0{\cdot}20$

The adopted metal abundances are not expected to be in error by such a large amount. The use of the GMA abundances for the metals results in values for $\Delta \log W_\lambda$ which are about one third the above values. The effects of further revisions in the metal abundances can be assumed to be even smaller. An error in $[\alpha]$ of about $\pm 0{\cdot}02$ can be anticipated.

A change in the metal abundance does not affect the abundance based on weak high excitation lines. This result contradicts a claim by Zwaan (1962) who applied to the GMA abundances for carbon, nitrogen and oxygen a uniform correction of $-0{\cdot}10$ dex because their assumed metal abundances were too low. This correction should be applied only to lines formed in the outer layers in which the metal ionization is the dominant source of electrons. In the deeper layers ($\log \tau_0 \geqslant 0$) hydrogen ionization is dominant. Since the N I lines are formed in these layers, Zwaan's correction should not be applied to the N I abundance.

Finally, to illustrate the importance of accurate abundances for the metals it will be pointed out that if all metal abundances were increased by a factor 5, the solution from the CH band would be in good agreement with results from the

other atomic and molecular spectra. The resultant abundance correction for carbon would be [C] = +0·1 instead of −0·15 as at present. The results for [N] and [O] would be little changed. The error in the revised abundance is certainly less than 50 per cent. A five-fold increase is an extreme case which highlights the need for accurate abundances.

14.2.4 *The helium abundance.* A helium abundance $A_{He} = 0{\cdot}09$ was assumed for the pressure calculations (Gaustad 1964). The predicted equivalent widths for molecular lines are independent of the helium abundance, Schadee (1964). The atomic lines are only weakly dependent on the assumed abundance; the correction corresponding to an increase to $A_{He} = 0{\cdot}20$ is only +0·03 dex. The conclusion is that the abundance errors resulting from an error in the helium abundance are negligible.

14.2.5 *Microturbulence.* A depth independent microturbulence of 1·8 km/s was adopted for the calculations (Waddell 1958). Schmalberger (1963) investigated the depth dependence of the microturbulence, and suggested that the observations were reproduced better if the radial component of the microturbulence increased inwards from about 1·4 km/s to 3·1 km/s in the deep layers with a fairly sharp transition region at about log $\tau_0 = 0{\cdot}4$. Anisotropic turbulence will not be considered because the present investigation is restricted to observations made at the centre of the disk.

Microturbulence affects the saturated portion of the curve of growth. The lines primarily affected by errors in the adopted microturbulence are the strong C I, O I, CN violet and CH lines. The sensitivity of the abundance to a change of ±0·5 km/s in the depth independent microturbulence was investigated: for a typical C I line Δ[C] = ∓0·05 and for O I λ7774 Δ[O] = ∓0·03. Similar corrections apply to the molecular lines. Next, the calculations were repeated for Schmalberger's microturbulent velocities. The C I lines are unaffected but for the weaker O I triplet λ7774, the correction Δ[O] = −0·06 is obtained.

It is concluded that errors of ±0·05 in [α] are introduced by uncertainties in the microturbulence. Accurate line profiles are required so that the microturbulence may be better defined. The abundances derived from the weak lines are independent of the assumed microturbulence.

14.2.6 *The continuous absorption coefficient.* The discussion is restricted to the effect of errors in the absorption coefficient of the negative hydrogen ion (H^-). Similar errors for the minor opacity sources (H, He^-, H_2^+) can be assumed not to be important.

The majority of the lines—atomic and molecular—occur in the wavelength region λ5000–10 000 Å. Over this interval bound–free transitions of H^- are the dominant source of opacity. Mutschlechner (quoted by Müller (1966)) compared theoretical equivalent widths based on the Chandrasekhar (1945) bound–free cross sections with those based on later computations by Geltman (1956). The differences did not exceed 3 per cent. Errors in the cross sections (Geltman 1962) adopted in this investigation are unlikely to exceed the above difference.

Errors in the H^- free–free absorption coefficient affect the abundances derived from the CO overtone bands at 2·35 microns. The absorption coefficients calculated

by Geltman (1965) were adopted. The author's estimated uncertainty corresponds to an abundance error of less than 2 per cent.

The total effect on the abundances of the likely errors in the continuous absorption coefficient is very small.

15. *The final abundances*

The final carbon, nitrogen and oxygen abundances are obtained directly from Figs 12(a), (b). The results are as follows:

$$\begin{aligned} [\mathrm{C}] &= -0{\cdot}17 \pm 0{\cdot}05 \text{ or } \log A_{\mathrm{C}} = -3{\cdot}45 \pm 0{\cdot}05 = 8{\cdot}55\text{–}12{\cdot}00 \\ [\mathrm{N}] &= -0{\cdot}05 \pm 0{\cdot}10 \quad \log A_{\mathrm{N}} = -4{\cdot}07 \pm 0{\cdot}10 = 7{\cdot}93\text{–}12{\cdot}00 \\ [\mathrm{O}] &= -0{\cdot}19 \pm 0{\cdot}05 \quad \log A_{\mathrm{O}} = -3{\cdot}23 \pm 0{\cdot}05 = 8{\cdot}77\text{–}12{\cdot}00 \end{aligned}$$

The uncertainty in log A is assessed on the basis of the scatter in Figs 12(a), (b).

In deriving the carbon abundance the CH band was discarded. The oxygen abundance is based on the strong permitted lines, the weak forbidden lines and a combination of the CO overtone bands and the permitted and forbidden carbon lines. The nitrogen abundance is the least accurate. The discrepancy between the weak and strong O I lines suggests that the temperature distribution for the deep layers could be in error. If this is correct the abundance from the N I lines should be reduced by about 0·10 dex, which would bring it into better agreement with the CN bands. On the other hand, the experimental oscillator strengths imply that [N] should be increased by about +0·10 dex over the result plotted in Fig. 12(b).

No useful purpose would be served by an extensive comparison with abundances obtained by other workers. The differences can be attributed to a variety of causes: the model atmospheres, oscillator strengths, equivalent widths, etc. However, it is of interest to repeat the principal reason why the present abundances differ from the GMA results. The model atmospheres are similar. For the atomic lines the coulomb approximation oscillator strengths were adopted in both cases. The one major difference is that line damping was included in the present investigation. Calculations for the O I λ7774 triplet including and excluding line damping were presented by Mugglestone & O'Mara (1965). These show that line damping is responsible for the abundance correction for these lines. The C I lines are stronger than the O I lines and the damping correction must, therefore, be larger. GMA noted that the infra-red C I lines gave an abundance which was larger than the averaged value obtained from all lines (see Section 6.3.1). Adopting the abundance from the infra-red lines, the correction is then [C] = −0·27, which is larger than [O]. Finally, the weak N I lines are insensitive to the damping constant and, indeed, [N] = −0·05 is obtained.

It is instructive to compare the revised abundances with the measurements of the abundance ratios obtained from solar cosmic rays (Biswas & Fichtel 1964). Simple theoretical arguments suggest that, in solar cosmic rays, the abundance ratios for nuclei with the same charge-to-mass ratio will be preserved during both the acceleration phases in a solar flare and the passage to the Earth. Confirmation of this expectation is provided by the observation that the abundance ratios are identical in the observed events. Biswas & Fichtel demonstrated that the abundance ratios were in good agreement with the ratios obtained from the GMA abundance determinations.

The abundances given by the present analysis lead to the following ratios

$$\frac{N_C}{N_O} = 0{\cdot}60 \pm 0{\cdot}10 \text{ and } \frac{N_N}{N_O} = 0{\cdot}15 \pm 0{\cdot}05$$

which are in satisfactory agreement with the cosmic ray measurements which give

$$\frac{N_C}{N_O} = 0{\cdot}59 \pm 0{\cdot}07 \text{ and } \frac{N_N}{N_O} = 0{\cdot}19 \pm 0{\cdot}04.$$

This agreement lends additional weight to the suggestion that the abundances in the solar cosmic rays are representative of the photospheric material. The significance of this suggestion is that it enables the abundances of the spectroscopically inaccessible elements—helium and neon—to be derived. The determination by this method and a discussion of the helium and neon abundances is reported elsewhere (Lambert 1967 b, c).

16. *Concluding remarks*

The initial motivation for this study was a desire to provide a comprehensive discussion of the abundances of carbon, nitrogen, and oxygen which was based on the molecular as well as the atomic spectra.

This paper has shown that the molecular spectra can be used successfully for abundance analyses. Further, the combination of molecular and atomic spectra provides especially valuable evidence on the absolute intensity of the solar continuous spectrum, see Section 14.2.1.

The problems involved in an abundance determination are the familiar ones: lack of accurate oscillator strengths, uncertainties in the model atmosphere, inaccurate equivalent widths, etc. Although further improvements in these essential items are to be welcomed—especially in the atomic oscillator strengths and molecular dissociation energies—a reappraisal of the approach to abundance analyses will soon be the most urgent need. The information contained in the line profiles and in their centre–limb variation must be tapped. For example, the reason for the apparent discrepancy between the weak and strong O I lines might be discovered by an analysis of their centre–limb variation. A detailed investigation of the line profiles across the disk would yield much information about the solar atmosphere in addition to the abundance of the element.

Acknowledgments. The writer is indebted to Professor D. E. Blackwell for reading and commenting upon the manuscript. He is indebted to Professor Blackwell and Mr E. A. Mallia for permission to quote their unpublished equivalent width measurements. He also wishes to thank Dr B. Warner for the use of a computer programme to calculate coulomb approximation oscillator strengths, and for permission to quote the results of unpublished calculations. Helpful correspondence with Drs Baschek, Cowley and Schadee is gratefully acknowledged.

Department of Astrophysics,
Oxford.
1967 *June.*

References

Allen, C. W., 1938. *Astrophys. J.*, **88**, 125.
Aller, L. H., 1963. *The Atmospheres of Sun and Stars*, Ronald Press, New York.
Arpigny, C., 1966. *Mem. Soc. r. Sci. Liège*, Ser. 5, **12**, 155.

Babcock, H. D. & Moore, C. E., 1947. *The Solar Spectrum, λ6600 to λ13495*, Carnegie Institute., Washington.
Ballik, E. A. & Ramsey, D. A., 1959. *J. chem. Phys.*, **31**, 1128; 1963. *Astrophys. J.*, **137**, 61.
Baschek, B., 1963. *Z. Astrophys.*, **56**, 207.
Bates, D. R. & Damgaard, A., 1949. *Phil. Trans. R. Soc.*, **A242**, 101.
Bennett, R. G. & Dalby, F. W., 1960. *J. chem. Phys.*, **32**, 1716; 1962. *J. chem. Phys.*, **36**, 399.
Berkowitz, J., 1962. *J. chem. Phys.*, **36**, 2533.
Biswas, S. & Fichtel, C. E., 1964. *Astrophys. J.*, **134**, 941.
Blackwell, D. E., Petford, A. D. & Mallia, E. A., 1967. *Mon. Not. R. astr. Soc.*, **136**, 365.
Brewer, L., Hicks, W. R. & Krikorian, O. H., 1962. *J. chem. Phys.*, **36**, 182.
Brewer, R. G. & Kester, F. L., 1964. *J. chem. Phys.*, **40**, 812.
Carroll, P. K., 1956. *Can. J. Phys.*, **34**, 83.
Chandrasekhar, S., 1945. *Astrophys. J.*, **102**, 223, 395.
Childs, D. R., 1964. *J. quant. Spectrosc. radiat. Transfer*, **4**, 283.
Chupka, W. A. & Ingram, M. G., 1955. *J. phys. Chem.*, **59**, 100.
Clementi, E., 1960. *Astrophys. J.*, **132**, 398.
Cowley, C. R., 1964. *Astrophys. J.*, **139**, 1344; 1966. Personal communication.
Davis, S. P. & Phillips, J. G., 1963. *The Red System ($A^2\Delta$–$X^2\Pi$) of the CN Molecule*, University of California Press, Berkeley.
Delbouille, L. & Roland, G., 1963. *Photometric Atlas of The Solar Spectrum from λ7498 to λ12016*, Liège.
Doherty, L. R., 1961. Thesis, University of Michigan.
Edmonds, F. N., 1962. *Astrophys. J. Suppl. Ser.* **6**, 357.
Eriksson, K. B. S., 1958. *Ark. Fys.*, **13**, 429.
Eriksson, K. B. S., 1965. *Ark. Fys.*, **30**, 199.
Eriksson, K. B. S. & Isberg, H. B. S., 1963. *Ark. Fys.*, **24**, 549.
Fairbairn, A. R., 1964. *AIAA J.*, **2**, 1004; 1966. *J. quant. Spectrosc. radiat. Transfer*, **6**, 325.
Faulkner, D. J. & Mugglestone, D., 1962. *Mon. Not. R. astr. Soc.*, **124**, 11.
Foster, E. W., 1962. *Proc. Phys. Soc.*, **79A**, 94; 1962. *Proc. Phys. Soc.*, **80A**, 882.
Froese, C., 1966. *Astrophys. J.*, **145**, 932.
Garstang, R. H., 1951. *Mon. Not. R. astr. Soc.*, **111**, 115; 1956. *The Airglow and the Aurorae*, p. 324, Pergamon Press, London.
Gaustad, J. E., 1964. *Astrophys. J.*, **139**, 406.
Geltman, S., 1956. *Phys. Rev.*, **104**, 346; 1962. *Astrophys. J.*, **136**, 935; 1965. *Astrophys. J.*, **141**, 376.
Goldberg, L., McMath, R. R., Mohler, O. C. & Pierce, A. K., 1952. *Phys. Rev.*, **85**, 140, 481.
Goldberg, L., Müller, E. A. & Aller, L. H., 1960. *Astrophys. J., Suppl. Ser.*, **5**, 1.
Hagen, L. G., 1963. University of California Radiation Laboratory Report 10620.
Harrington, J. A., Modica, A. P. & Libby, D. R., 1966. *J. chem. Phys.*, **44**, 3380.
Herzberg, G., 1950. *Spectra of Diatomic Molecules*, Van Nostrand, New York; 1957. *Mem. Soc. r. Sci. Liège*, **18**, 397.
Hicks, W. T., 1957. University of California Radiation Laboratory Report 3696.
Houziaux, L., 1961. *Z. Astrophys.*, **53**, 237.
de Jager, C. & Neven, L., 1957. *Mem. Soc. r. Sci. Liège*, **18**, 357; 1964. *Mem. Soc. r. Sci. Liège, Ser.* 5, **9**, 213.
de Jager, C., Heintze, J. R. W. & Hubenet, H., 1964. *Bull. astr. Insts Neth.*, **17**, 442.
Jeunehomme, M., 1965. *J. chem. Phys.*, **42**, 4086.
Jeunehomme, M. & Schwenker, R. P., 1965. *J. chem. Phys.*, **42**, 2406.
Johansson, L., 1963. *Ark. Fys.*, **25**, 425; 1966. *Ark. Fys.*, **31**, 201.
Johansson, L. & Litzen, U., 1965. *Ark. Fys*, **29**, 175.
Jürgens, G., 1954. *Z. Phys.*, **138**, 613.
Kelly, P. S., 1964. *J. quant. Spectrosc. radiat. Transfer*, **4**, 117.
Knight, H. T. & Rink, J. P., 1962. *J. chem. Phys.*, **35**, 199.
Kundryavtsev, E. M., Gippius, E. F., Derbeneva, S. S., Pechenov, A. N. & Sovolev, N. N., 1963. *High Temp.*, **1**, 338.
Laborde, G., 1961. *Ann. Astrophys.*, **24**, 89.

Labs, D. & Neckel, H., 1962. *Z. Astrophys.*, **55**, 269; 1963. *Z. Astrophys.*, **57**, 283.
Lambert, D. L., 1965. Thesis, University of Oxford.
Lambert, D. L., 1967a. In preparation.
Lambert, D. L., 1967b. *Nature, Lond.*, **215**, 43.
Lambert, D. L., 1967c. *Observatory*, in press.
Lambert, D. L. & Swings, J. P., 1967a. *Sol. Phys.*, **2**, 34; 1967b. *Observatory*, **87**, 113.
Lambert, D. L. & Warner, B., 1967. In preparation.
Le Blanc, F. J., Oldenburg, O. & Carleton, N. P., 1966. *J. chem. Phys.*, **45**, 2200.
Maecker, H., 1953. *Z. Phys.*, **135**, 13; 1956. *Z. Naturf.*, **11**, 457.
Makarova, E. A., 1964. *Astr. J., N.Y.*, **8**, 222.
Mallia, E. A. & Blackwell, D. E., 1967. Personal communication.
Mallia, E. A., 1967. Personal communication.
Mastrup, F. & Wiese, W. L., 1958. *Z. Astrophys.*, **44**, 259.
Mohler, O. C., 1955. *A Table of Solar Spectrum Wavelengths* 11984 *A to* 25578 *A*, University of Michigan Press, Ann Arbor.
Moore, C. E. & Broida, H. P., 1959. *J. Res. natn Bur. Stand.*, **63A**, 19.
Mugglestone, D. & O'Mara, B. J., 1965. *Mon. Not. R. astr Soc.*, **129**, 41.
Müller, E. A., 1966. *Abundance Determinations in Stellar Spectra*, p. 171, I.A.U. Symposium No. 26, Academic Press, New York.
Newkirk, G., 1957. *Astrophys. J.* **125**, 571.
Pecker, J. C. & Peucheot, M., 1957. *Mem. Soc. r. Sci. Liège*, **18**, 352.
Petrie, W., 1950. *J. geophys. Res.*, **55**, 143.
Reis, V. H., 1965. *J. quant. Spectrosc. radiat. Transfer*, **5**, 585.
Richter, J., 1958. *Z. Phys.*, **151**, 114; 1961. *Z. Astrophys.*, **51**, 177.
Rigutti, M., 1962. *Publs Dom. Obs.*, **25**, No. 2.
Rigutti, M. & Drago-Chiuderi, F., 1963. *Ann. Astrophys.*, **26**, 253.
Rigutti, M. & Poletto, G., 1965. *Z. Astrophys.*, **60**, 199, 289.
Schadee, A., 1964. *Bull. astr. Insts Neth.*, **17**, 311; 1967. *J. quant. Spectrosc. radiat. Transfer*, **7**, 169.
Schmalberger, D. C., 1963. *Astrophys. J.*, **138**, 693.
Shidei, T., 1936. *Jap. J. Phys.*, **11**, 23.
Solarski, J. & Wiese, W. L., 1964. *Phys. Rev.*, **135A**, 1236.
Spindler, R., 1965. *J. quant. Spectrosc. radiat. Transfer*, **5**, 165.
Stephenson, G., 1951. *Proc. phys. Soc.*, **A64**, 666.
Sviridov, A. G., Sobolev, N. N. & Sutovskii, E. M., 1965. *J. quant. Spectrosc. radiat. Transfer*, **5**, 525.
Sviridov, A. G., Sobolev, N. N. & Novgorodov, M. Z., 1966. *J. quant. Spectrosc. radiat. Transfer*, **6**, 337.
Sviridov, A. G., Sobolev, N. N., Novgorodov, M. Z. & Arutyunova, G. A., 1966. *J. quant. Spectrosc. radiat. Transfer*, **6**, 875.
Swings, J. P., 1966. *Ann. Astrophys.*, **29**, 371.
Tatum, J. B., 1967. *Astrophys. J., Suppl. Ser.*, in press.
Thomas, R. N. & Athay, R. G., 1961. *Physics of the Solar Chromosphere*, p. 178, Interscience, New York.
Tsuji, T., 1964. *Ann. Tokyo astr. Obs.*, **9**, 1.
Utrecht Observatory Staff, 1960. *Rech. astr. Obs. Utrecht*, **1**, 5.
Varsavsky, C. M., 1958. Thesis, Harvard University.
Waddell, J. H., 1958. *Astrophys. J.*, **127**, 284.
Warner, B., 1967. Personal communication.
Wiese, W. L., Smith, M. W. & Glennon, B. M., 1966. *Atomic Transition Probabilities*, Vol. 1, National Bureau of Standards, Washington.
Wilkinson, R. G., 1963. *Astrophys. J.*, **138**, 778.
Young, L. A. & Eachus, W. J., 1966. *J. chem. Phys.*, **44**, 4195.
Zwaan, C., 1962. *Bull. astr. Insts Neth.*, **16**, 225.